AN ABSTRACT OF THE THESIS OF

Brandon J. Barrett for the degree of Master of Science in Chemical Engineering presented on May 17, 2002.
Title: Molecular and Rheological Characterization of Hyaluronic Acid: Determination of its Role in Thrombin-Catalyzed Fibrin Clotting and Viscosupplementation of Joints

Redacted for privacy

Abstract approved_____
Willie E. Rochefort

Three samples of the biopolymer hyaluronic acid (HA) were characterized in the following manner: the molecular weights were obtained via multi-angle laser light scattering; the intrinsic viscosities were calculated through dilute solution viscometry, and the rheology of HA solutions was determined with constant rate rotational viscometry and dynamical mechanical testing.

In addition, the highly debated role of hyaluronic acid in wound healing was examined by studying the effect that HA has upon thrombin-catalyzed fibrin clotting. Fibrin, in phosphate-buffered saline, was clotted both alone and after being incubated with HA. It was determined that the presence of hyaluronic acid resulted in a slower clotting process; in effect, HA acts as an anti-coagulant. Based upon the experimental evidence, it is proposed that this anti-coagulant phenomenon

arises through a combination of two mechanisms: 1) specific binding between HA and fibrin, which acts to retard fibrin clotting through steric hindrance, and 2) the formation of an HA network which slows fibrin clotting by hindering free diffusion of fibrin and thrombin.

Finally, creation of a synthetic replacement for synovial fluid was attempted using xanthan gum and locust bean gum in phosphate-buffered saline. The phenomenon of gum synergism was utilized in an effort to exert some degree of fine-tuning over the final rheological properties of the solution. This also would provide the side benefit of reducing the weight of gum required per unit volume. By mixing the solutions at different temperatures, it was possible to exploit the tendency of xanthan gum to uncoil at higher temperatures and therefore bind more strongly to locust bean gum. However, it was determined that no combination of gum concentrations and processing conditions resulted in a gum solution that adequately mimicked the rheology of a hyaluronan solution.

Molecular and Rheological Characterization of Hyaluronic Acid: Determination of its Role in Thrombin-Catalyzed Fibrin Clotting and Viscosupplementation of Joints

by
Brandon J. Barrett

A THESIS

submitted to

Oregon State University

in partial fulfillment of
the requirements for the
degree of

Master of Science

Presented May 17, 2002
Commencement June 2003

Master of Science thesis of Brandon J. Barrett presented on May 17, 2002.

APPROVED:

Redacted for privacy

Major Professor, representing Chemical Engineering

Redacted for privacy

Head of the Department of Chemical Engineering

Redacted for privacy

Dean of the Graduate School

I understand that my thesis will become part of the permanent collection of Oregon State University libraries. My signature below authorizes release of my thesis to any reader upon request.

Redacted for privacy

Brandon J. Barrett, Author

ACKNOWLEDGMENTS

I'd like to thank Hai Le, Stephanie Hobbs, Neil Geisler, and Meghaan Smith for their help with data collection, and Stephanie Solarz for proofreading several edits of the manuscript, as well as giving moral support throughout the project.

Thanks to Dr. Cindy Bower for providing her phosphate-buffered saline recipe, as well as the ingredients to make it, and to Drs. Goran Jovanovic, Michelle Bothwell and Bernd Simoneit for agreeing to serve on my graduate committee.

Finally, I'd like to show my appreciation to Dr. Skip Rochefort, who has been my mentor in chemical engineering for going on seven years. His advice, constructive criticism, and ample supply of viscoelastic toys were instrumental in getting this work down on paper.

TABLE OF CONTENTS

TABLE OF CONTENTS (continued)

LIST OF FIGURES

LIST OF FIGURES (continued)

LIST OF FIGURES (continued)

LIST OF TABLES

MOLECULAR AND RHEOLOGICAL CHARACTERIZATION OF HYALURONIC ACID: DETERMINATION OF ITS ROLE IN THROMBIN-CATALYZED FIBRIN CLOTTING AND VISCOSUPPLEMENTATION OF JOINTS

1. INTRODUCTION

This thesis is a union of three distinct chapters with the following themes: 1) the molecular and rheological characterization of hyaluronic acid solutions, 2) the effect of hyaluronic acid upon the rate of thrombin-catalyzed fibrinogen clotting, and 3) a study of synergistic and temperature-related effects on various mixed polysaccharide gum solutions. While these may appear to be somewhat disparate topics, there is an important underlying theme which ties the chapters together: the use of hyaluronic acid as a therapeutic in human medicine.

As will later be discussed in more detail, hyaluronic acid is an important component of the synovial fluid found encapsulated within the large articular joints of the human frame (e.g. the knee). It has been demonstrated that hyaluronic acid (HA) is largely responsible for the unique rheological properties of synovial fluid, which allows for both sliding flow and elastic flow. Quite simply, HA solutions work well as both lubricants and shock-absorbers, depending on the nature of the forces upon them.

It may be expected, therefore, that a degradation of HA would result in a deleterious condition of the joint. In support of this theory, studies show that patients presenting with osteoarthritis have markedly reduced concentrations of HA in their synovial fluid, and that the HA which is present is of lower than normal molecular weight. (The root cause of this degradation has variously been attributed to factors from mechanical injury to an excess of free radicals.) Given this, it should come as no surprise that viscosupplementation—the injection of high-molecular weight hyaluronic acid into the affected joint—is a proven therapy for osteoarthritis.

In order to engineer the most cost-efficient, therapeutically-effective HA viscosupplementation solution, it is crucial that the link between HA's molecular properties and its rheological performance be fully understood. While some efforts have been made in this direction, Chapter Two of this thesis provides an integrated study of form vs. function that has not yet been attempted. Using three samples of HA from the same source and supplier, each with different molecular weights, it is possible to directly relate molecular properties to rheological performance. Low-angle laser light scattering was used to precisely determine molecular weights, dilute solution viscometry to characterize extent of networking, and rheological tests to determine flow curves and viscoelastic behavior.

However, the usefulness of HA may not be confined to viscosupplementation. Many researchers believe that HA is far more than an inert "stuffing" for the joints, and may play an active role in several biological processes. In particular, the notion that HA is a participant in the cascade process that leads to fibrin clotting has received a fair amount of attention, due to the potentially useful applications that could result from such studies. A solution that increased the rate of fibrin clotting could work to enhance wound healing; a solution that decreased the rate could work to prevent tissues from adhering to one another during surgeries. Yet thus far there is no consensus on exactly what role, if any, HA might play in wound healing.

Chapter Three discusses research that attempts to elucidate this relationship. Fibrin-clotting was activated by thrombin with and without the presence of hyaluronic acid, while clot formation was monitored via real-time elastic measurements of the resulting clotted mass. Using the characterization described in Chapter Two, it was possible to take a step further and relate HA molecular mass and degree of networking to its effect on fibrin clotting.

HA has the potential to be an extremely useful medical resource, but there is one drawback to its use that has proven formidable: cost. The three main sources of commercial HA are rooster combs, human umbilical cord, and bacterial

fermentation; in all three cases, extraction and purification of HA is a difficult and costly procedure. Hyaluronic acid is therefore an extremely expensive product, on the order of hundreds of dollars a gram, so it would be difficult for all but the wealthiest of consumers to justify the use of it on a regular basis. It may be feasible, however, to perform viscosupplementation procedures with injectible solutions that, although mimicking the rheological properties of synovial fluid, contain no HA whatsoever. Chapter Four relates work that attempted this feat with solutions of polysaccharide gums, which were chosen for their low cost, proven biocompatibility, and ability to interact with one another in a synergistic manner. Along with the concentration and molecular weights of the gums involved, this allows for another level of engineering control over the final solution properties.

However, given the extremely specialized nature of the biological roles that HA is suspected to play, it should be kept in mind that a mixed gum viscosupplement may be perfectly adequate in a purely mechanical sense but still fail to fill the biochemical niche filled by HA. This brings us back to the subject matter of Chapter Three: does HA in fact perform vital biological roles other than its rheological one? If so, will any large anionic polymers adequately perform these roles, or are the interactions of a more subtle biochemical nature? These are questions which remain to be answered as the field of applied HA research matures.

2. CHARACTERIZATION OF HYALURONIC ACID

2.1 INTRODUCTION

Hyaluronic acid is a biopolysaccharide (see Figure 2.1) ubiquitous throughout the body but found in significant concentrations only in a handful of specialized structures (e.g. the knee joint and umbilical cord). Since the discovery of HA there have been scattered attempts at its characterization, for the most part focusing either upon the rheological behavior of HA solutions or the molecular weight and configuration of the molecule. Few integrated studies correlating molecular weight and size to rheological characteristics have been performed; in fact, most studies on the rheology of HA neglect to even mention the source and molecular weight of the samples used—probably because this information is not at hand. Fouissac, Milas and Rinaudo (1993) have provided maybe the most complete attempt of HA characterization to date, but concentrated solely on determining the viscosity of HA solutions as a function of shear rate, and reported no viscoelastic data. On the other hand, Wik and Wik (1998) provide a good review of HA viscoelasticity, but fail to give similar attention to the molecular side of the equation.

The usefulness of HA stems from *both* its solution viscosity and its viscoelasticity, which are both intimately tied to molecular weight and configuration. If researchers are to have a good working knowledge of the biopolymer, sufficient to

allow the creation of tailor-made HA solutions for specific uses, then the relationships between these variables must be well-understood.

By performing rheological measurements on HA of measured molecular weight and measured intrinsic viscosity, this author was able to provide an overview of these relationships.

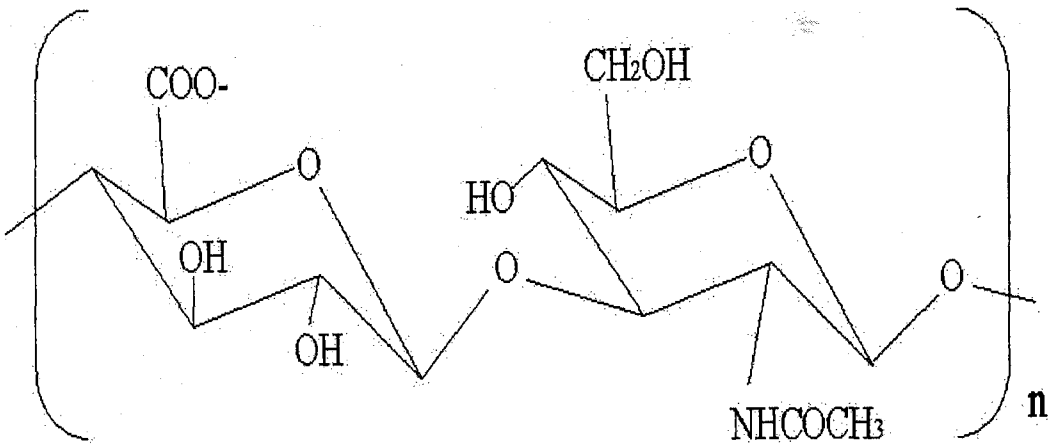

FIGURE 2.1: Structure of the hyaluronic acid repeat unit

2.2 LITERATURE REVIEW

The solvent basis of synovial fluid is blood plasma, and the composition of synovial fluid would be virtually indistinguishable from that solvent were it not for the presence of the macromolecule which has been variously termed hyaluronic acid, sodium hyaluronate, and hyaluronan. In a healthy knee, the concentration of hyaluronic acid (HA) is in the vicinity of 3.5 mg/ml (Balazs, 1982), with a molecular weight of approximately 1.6 - 2 x 10^6 (Cowman et al., 1998).

While the flow properties of synovial fluid have been investigated since the early 1950's, the first published study on the rheology of isolated hyaluronan was that of Gibbs, Merrill and Smith (1968), which was dedicated to dynamic viscoelastic properties. HA of a single molecular weight (2.8 x 10^4 as determined by short-column sedimentation equilibrium measurements) was used in all experiments. The storage and loss moduli of HA solutions were measured on an oscillating Couette rheometer, with an eye toward determining the effects that pH (1.5 to 7), temperature (3.5 to 25° C), polymer concentration (2.1 to 4 mg/ml), and ionic strength (0 N NaCl to 0.2 N NaCl) have upon them. It was determined that while changing the above parameters did affect the resulting moduli curves, it only served to shift them along the time axis; the shapes of the curves are unaffected.

Because Gibbs, Merrill and Smith confined their studies, for the most part, to solution parameters that are not encountered *in vivo*, their specific results are not relevant to this paper. It may be useful to consider the implications that can be arrived at regarding molecular structure; however, since the shape of the moduli curves are unchanged by moderate shifts in pH, temperature, polymer concentration, and ionic strength, it is clear that these factors affect only the relaxation rate and not the actual mechanism at work. One can therefore rule out the creation of intermolecular crosslinks, the onset of polymer degradation, or any other actions that would result in fundamental changes in the mechanism of relaxation. It would appear from these studies that the viscoelastic behavior of HA solutions is unaffected by moderate shifts in solution parameters. Also note that because the study involved only a single molecular weight—and a relatively low one at that—it may be somewhat difficult to draw generalizations from this data.

Fouissac, Milas and Rinaudo (1993) have helped elucidate the effects that shear rate, molecular weight, and concentration have upon the viscosity of HA solutions. They obtained HA samples over a range of molecular weights as provided by ARD Co., and then determined the weight average molecular weight of the samples via steric exclusion chromatography. Flow curves were obtained on Contraves LS 30 and Carrimed CS 50 rheometers, and intrinsic viscosities were also measured, although the method of measurement is not explicitly given in the paper.

Fouissac et al. (1993) found that in all respects, the dependencies of HA were considerably different from most flexible polymers in solution. These differences can be summarized as follows: 1) HA solutions show entanglement effects at relatively low concentrations—about 10 times lower than expected for a flexible polymer. 2) The zero-shear viscosity of HA solutions show a greater dependence on molecular weight than expected: M^4 rather than $M^{3.4}$. 3) Shear-thinning behavior appears at relatively low rates of shear, especially at higher HA concentrations. At 0.01 g/ml, for example, shear-thinning appears at 0.1 s^{-1}, while at 0.002 g/ml shear-thinning does not appear until approximately 100 s^{-1} (MW = 135 000 as determined by steric exclusion chromatography).

The work of Fouissac and his colleagues (1993) prompted much research into the rheology of HA solutions. The most comprehensive rheological study to date is, arguably, that presented by Wik and Wik (1998). While lacking the rigorous molecular characterization that Fouissac et al. (1993) attempted, such as determination of the critical overlap concentration, Wik and Wik's paper does present data regarding the zero shear viscosity, shear thinning behavior, and viscoelasticity of HA solutions. They found that HA chains begin to entangle at relatively low concentrations; on a graph of viscosity versus concentration (mg/ml) times molecular mass (CM), the curve shows two distinct straight-line regions representing the dilute and the concentrated regimes of flow. When $CM \approx 2 \times 10^6$,

at which point the viscosity is 10 mPa*s, the slope of the curve increases dramatically, signaling the onset of entanglement.

Wik and Wik's experiments on shear thinning found that the viscosity of a 1wt% solution of hyaluronic acid ($M_r = 4.3 \times 10^6$) drops from a zero shear viscosity of 400 000 mPa*s to 130 mPa*s at a shear rate of 10^3 s^{-1}. This behavior remains consistent for solutions of HA of differing molecular weight, though lower molecular weight HA shows lower initial viscosity (e.g. at 10^{-3} s^{-1}, HA, $M_r = 670$ 000, shows a viscosity of 400 mPa*s, while HA, $M_r = 4.3 \times 10^6$, shows a viscosity of 400 000 mPa*s). The curves of high MW HA and low MW HA begin to converge at higher rates of shear, however, until there is essentially no difference between any of them at 10^3 s^{-1}. At this shear rate it would appear that the hyaluronic acid molecules have become fully elongated within the flow, rendering their molecular weight more or less irrelevant with regards to solution viscosity.

Wik and Wik (1998) note the practical implications of this extreme shear-thinning behavior: solutions of hyaluronic acid can be easily delivered via syringe because the high rate of shear within the cannulas results in a relatively low viscosity. Wik and Wik's study of viscoelasticity supports the work of Gibbs, Merrill and Smith (1968), though they present their results in a simplified form designed for the non-specialist, utilizing the concept of "percent elasticity, percent viscosity" rather

than storage and loss moduli. An ideal elastic material would therefore be 100% elastic, and an ideal viscous solution would be 100% viscous. Wik and Wik (1998) show that HA of low molecular weight (7×10^5) exhibits a predominantly viscous behavior over a range of applied frequencies: from 0.001 to 0.1 Hz the solution is nearly 100% viscous. As the applied frequency increases above 0.1 Hz, the solution begins to become more elastic, changing to approximately 70% viscous and 30% elastic at 10 Hz.

As the molecular weight increases, Wik and Wik (1998) show that elastic behavior begins to emerge at lower frequencies, with the plateau region of 100% viscous behavior becoming limited to a much smaller range of low frequencies. For example, their highest molecular weight HA (4.3×10^6) is 15% viscous, 85% elastic at 0.001 Hz, and approximately 20% viscous, 80% elastic at 10 Hz.

In comparison, Wik and Wik's data indicates that a cross-linked HA gel is 85% elastic, 15% viscous over almost the entire range from 0.001 Hz to 10 Hz. (Crosslinked HA products are generically referred to as *hylans*. This crosslinking can be carried out in various ways, such as using formaldehyde or divinyl sulfone to link the hydroxyl groups. [Balazs et al., 1987; Band, 1998])

2.3 EXPERIMENTAL BACKGROUND AND THEORY

2.3.1 Determination of Molecular Weight

2.3.1.1 Average Molecular Weight

All synthetic polymers and most biological polymers have a distribution of chain lengths (a condition known as polydispersity). As a consequence, the molecular weight of a polymer cannot be determined simply by dividing the sample weight by the number of moles in the sample; rather, the notion of an *average* molecular weight must be introduced.

The number-average molecular weight, M_n, is defined as:

$$M_n = \frac{W}{N} = \frac{\sum_{x=1}^{\infty} n_x M_x}{\sum_{x=1}^{\infty} n_x} = \sum_{x=1}^{\infty} \left(\frac{n_x}{N} \right) M_x \qquad \text{Eqn. 2-1}$$

where:

N = total number of moles in sample

n_x = moles of x-mer present in sample

M_x = molecular weight of x-mer

The weight-average molecular weight, M_w, is defined as:

$$M_w = \sum_{x=1}^{\infty}\left(\frac{w_x}{W}\right)M_x = \frac{\sum n_x M_x^2}{\sum n_x M_x} \qquad \text{Eqn. 2-2}$$

where:

w_x = total weight of x-mer in sample

W = total weight of sample

Note that the number-average molecular weight is the first moment of the distribution (analogous to the center of gravity in mechanics), and the weight-average molecular weight is the second moment of the distribution (analogous to the radius of gyration in mechanics). The z-average molecular weight, the third moment of the distribution, is similarly defined and occasionally finds usage. Both methods of quantifying molecular weight are equally valid, though the weight-average molecular weight will always be higher than the number-average molecular weight for any given polydisperse polymer sample, due to the higher weighting of larger molecules.

In fact, the ratio M_w/M_n is often defined as the *polydispersity index*, where a polydispersity index of 1 indicates the unusual case where $M_w = M_n$. This indicates

that all polymer chains in the sample are of equal length, a condition known as monodispersity. More frequently the polydispersity index will be greater than one, indicating a distribution of molecular weights. Some commercial polymers have polydispersity indices of 50 or higher (Rosen, 1993).

2.3.1.2 Low Angle Laser Light Scattering (LALLS)

One technique commonly used to measure the average molecular weight of a polymer sample is light scattering. A laser beam passing through a solution will scatter at an intensity proportional to the product of the concentration and molecular weight of the solute. The quantitative nature of the relationship was determined by Zimm (1948), following the early work by Einstein (1910), Raman (1927) and Debye (1944):

$$R_\theta = K^* M_w c P(\theta)[1 - 2A_2 M_w P(\theta) c] \qquad \text{Eqn. 2-3}$$

where:

$R(\theta)$ = excess Rayleigh ratio; intensity of scattering of a molecular solution over the intensity of scattering of the solvent alone

M_w = weight averaged molecular weight

c = concentration

A_2 = second virial coefficient (measure of solvent-solute interaction)

$P(\theta)$ = scattering function which relates the angular variation in scattering intensity to mean square radius of particle, given by:

$$P(\theta) = 1 - \frac{16\pi^2}{3\lambda^2}\sin^2\left(\frac{\theta}{2}\right)\left\langle r_g^2 \right\rangle + \cdots \qquad \text{Eqn. 2-4}$$

where r_g is the root mean square radius of a particle.

K^* = collection of constants defined as:

$$K^* = \frac{4\pi^2\left(\frac{dn}{dc}\right)^2 n_o^2}{N_o\lambda_o^4} \qquad \text{Eqn. 2-5}$$

where:

dn/dc = refractive index increment of solution

n_o = refractive index of solvent

λ_o = wavelength of incident light in a vacuum

N_a = Avogadro's number

Equation 2-3 is often recast in the following form, known as the Zimm formalism:

$$\frac{K^* c}{R(\theta)} = \frac{1}{MP(\theta)} + 2A_2 c \qquad \text{Eqn. 2-6}$$

All terms on the left hand side of Equation 2-6 are known or measured quantities. On the right hand side are the terms which the experiment is designed to determine: M, the molecular weight, A_2, the second virial coefficient, and r_g, the root mean square radius, which is embedded in the scattering function.

If the low angle limit of the Zimm formalism is taken, the result is:

$$\frac{K^* c}{R(0)} = \frac{1}{M} + 2A_2 c \qquad \text{Eqn. 2-7}$$

since $P(0^\circ) \rightarrow 1$. The above equation is linear, with a y-intercept at 1/M and a slope of $2A_2$. By taking the low angle limit, the intermolecular scattering effects are eliminated.

If the low concentration limit of the Zimm formalism is taken, the result is:

$$\frac{K^* c}{R(\theta)} = -(\cdots)\langle r_g^2 \rangle \sin^2\left(\frac{\theta}{2}\right) + \frac{1}{M} \qquad \text{Eqn. 2-8}$$

Again, the equation is linear with a y-intercept at 1/M. The slope in this case is related to the root mean square radius. By taking the low concentration limit, the intramolecular scattering effects are eliminated.

It is apparent that if the experiment is run at several concentrations, and the scattering intensity is measured at several different angles at each concentration, then a double extrapolation to zero angle and zero concentration will provide all of the unknown quantities on the right hand side of Equation 2-6.

In practice, modern light scattering devices feature a pedestal on which a glass vial of solution will rest. A laser is beamed through the vial, and photodiodes, set at various angles around the pedestal, measure the intensity of scattered light. The user replaces the vial several times with different concentrations of solution, thus providing the basis for the extrapolation to zero concentration. (Since the hardware measures multiple angles for each concentration, the basis for extrapolation to zero angle is "built-into" the nature of the experiment.)

If the experiment is carried out correctly and carefully, the plotted results should be similar to Figure 2.2. Note that both sets of extrapolated data should intercept the y-axis at $1/M_w$. The second virial coefficient can be backed out from the slope of the projected zero angle line, and the root mean square radius can be backed out from the slope of the projected zero concentration line.

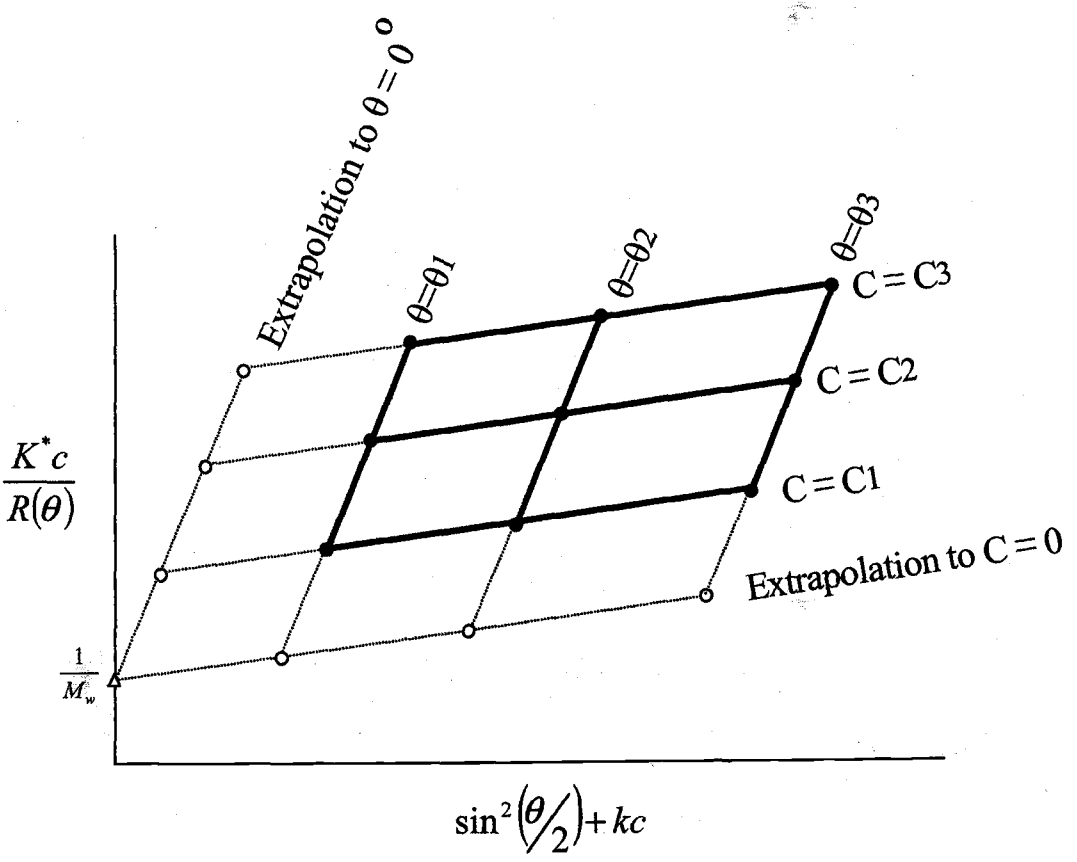

FIGURE 2.2: Example of a Zimm plot

The quantity k in the abscissa is known as the stretch factor; it is chosen in order to put the concentration term and the sine term in the same approximate numerical range, the purpose being to provide for a more legible plot. The choice of k does not affect the final results in any quantitative way.

The reader should note at this point that the molecular weight obtained via this method is necessarily an *average* molecular weight; in this case, the weight-average molecular weight is obtained. This may be sufficient for studies concerning monodisperse polymers, or for relative characterization of polydisperse samples. If more detailed information concerning the molecular weight distribution of a sample is required, then the light scattering analysis can be coupled with size-exclusion chromatography.

In this case, the pedestal described above is replaced with a flow cell through which the solution can pass (see Figure 2.3). The nature of the light scattering phenomenon itself is unchanged, although the refractive index of the glass cell now must be taken into account.

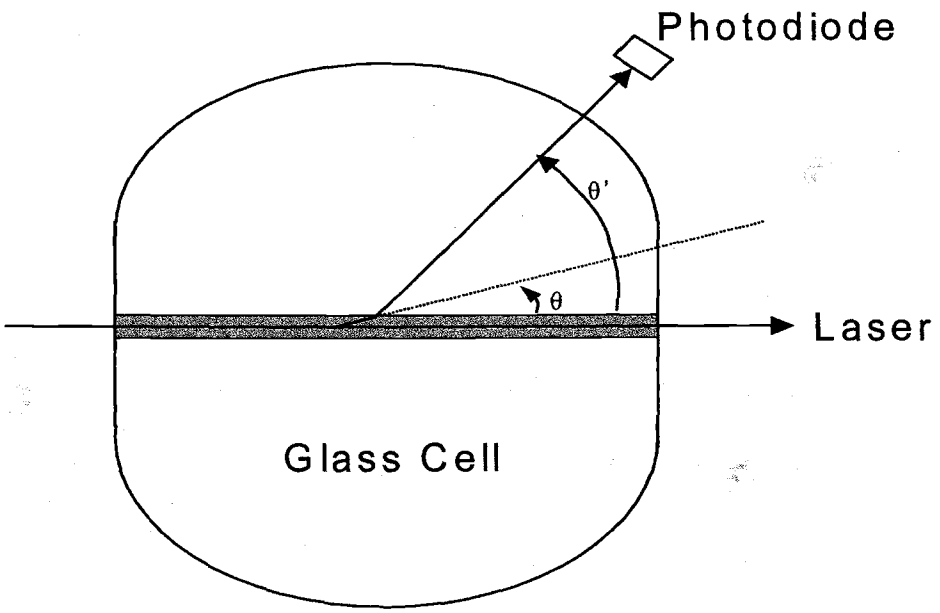

FIGURE 2.3: Schematic representation of flow cell

A typical light-scattering/SEC set-up is portrayed in Figure 2.4. Note that a SEC column is placed before the light scattering device in order to provide for separation of the polymer sample by size; under normal conditions the user may safely assume that the light scattering device is seeing a progression of essentially monodisperse samples. In order to retrieve concentration data from the sample, a DRI or UV detector is placed in-line after the light scattering device. If the liquid volume present in the line between the light scattering device and the concentration detector is measured, then the output from the two devices can be accurately aligned.

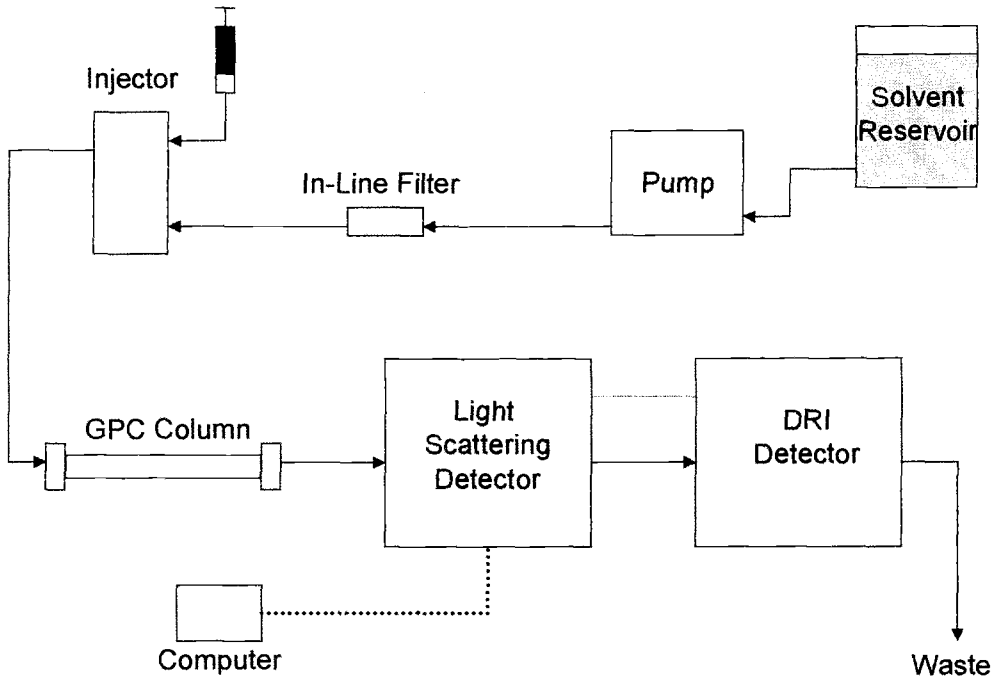

FIGURE 2.4: Typical LALLS/SEC experimental set-up

At any given time, then, the light scattering device has access to concentration data and scattering intensities at several angles for what is, hopefully, a monodisperse sample passing through the flow cell. This data can be used to produce a Debye plot as shown in Figure 2.5. Note that, due to the nature of the experiment, multiple concentrations are not available and so only a single concentration is used; because of this, the second virial coefficient is not available for determination, though the root mean square radius can still be calculated for each monodisperse element.

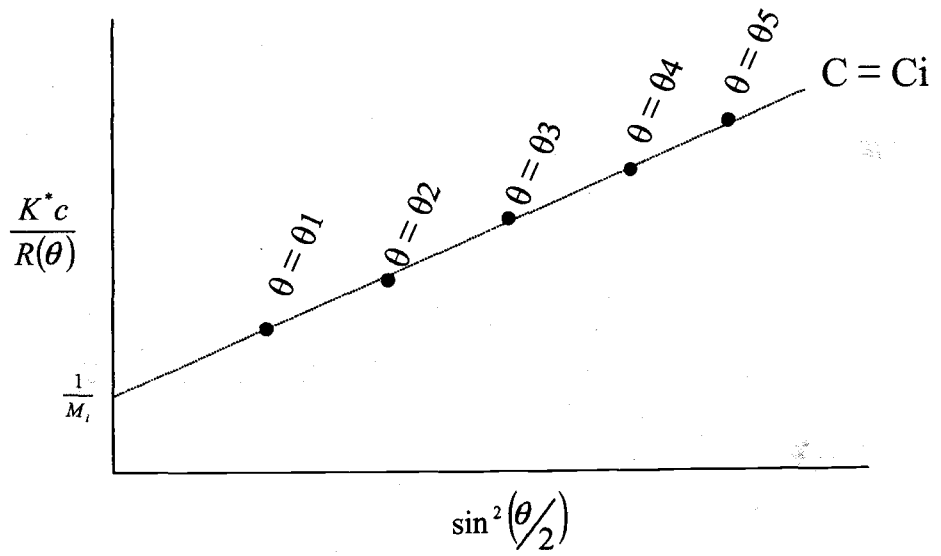

FIGURE 2.5: Example of Debye plot

It is now obvious that a weight-average molecular weight can be determined for as many "slices" of the eluted peak as is desired. If *i* slices are considered, and the Equations 2-1 and 2-2 for number- and weight-average molecular weight are rewritten as:

$$M_n = \frac{\sum c_i}{\sum \frac{c_i}{M_i}} \qquad \text{Eqn. 2-9}$$

$$M_w = \frac{\sum c_i M_i}{\sum c_i} \qquad \text{Eqn. 2-10}$$

$$M_z = \frac{\sum c_i M_i^2}{\sum c_i M_i} \qquad \text{Eqn. 2-11}$$

then it is clear that the user has access to all moments of the molecular weight distribution.

2.3.2 Rheological Characterization

2.3.2.1 Intrinsic Viscosity

The viscosity of a polymer solution is dependant upon several variables: temperature, solute concentration, the presence of polymer entanglements, the viscosity of the solvent, the molecular weight of the polymer solute, the identities of the polymer and solvent and the nature of their interactions. In order to relate a viscosity measurement to the polymer molecular weight, many of the above variables must be eliminated.

In order to eliminate the effect of solvent viscosity, the specific viscosity, η_{sp}, is defined as:

$$\eta_{sp} = \frac{\eta - \eta_s}{\eta_s} = \frac{\eta}{\eta_s} - 1 \qquad \text{Eqn. 2-12}$$

Where η is the solution viscosity and η_s is the pure solvent viscosity. Furthermore, in order to account for solute concentration, the reduced viscosity is defined as:

$$\eta_{red} = \frac{\eta_{sp}}{c} \qquad \text{Eqn. 2-13}$$

where c is the solute concentration. The effect of entanglements may be removed by extrapolating to zero concentration:

$$[\eta] = \lim_{c \to 0} \frac{\eta_{sp}}{c} = \lim_{c \to 0} \frac{(\eta/\eta_s) - 1}{c} \qquad \text{Eqn. 2-14}$$

Where $[\eta]$ is the intrinsic viscosity, typically given in units of grams per deciliter or grams per milliliter. In practice, measurements of reduced viscosity are carried out at several different polymer concentrations, allowing for an extrapolation to zero concentration. The reduced viscosity that the solution would exhibit at zero concentration, according to this extrapolation, is the intrinsic viscosity. Because the effects of solvent viscosity, solute concentration, and entanglements have been removed, the intrinsic viscosity of a given polymer-solvent system, at a given temperature, is related only to the molecular weight of the polymer. One relationship that generally holds true is the Mark-Houwink-Sakurada equation:

$$[\eta] = KM^a \qquad \text{Eqn. 2-15}$$

Where M is the polymer molecular weight and K and a are constants specific to the polymer-solvent system.

In addition to providing information about molecular weight, the intrinsic viscosity of a polymer-solvent system can give information regarding polymer entanglements. The product of intrinsic viscosity and polymer concentration in solution ($C[\eta]$) is a representation of the effective hydrodynamic volume of the polymer in a solvent. When $C[\eta] \leq 1$, the solution may be considered *dilute*, in that the polymer chains are not interacting. At $C[\eta] = 1$, the solution is entering the so-called *semi-dilute* region, wherein the polymer chains are beginning to interact with each other. At $C[\eta] >> 1$, the solution has entered the *concentrated* regime, and polymer chains are not simply interacting but are actually becoming entangled with each other. The concentration at which interactions between polymer molecules are just starting to become evident (that is, when the solution is entering the semi-dilute regime) is termed the *overlap concentration*, and is defined as:

$$C^* = \frac{1}{[\eta]} \qquad \text{Eqn. 2-16}$$

Intrinsic viscosity measurements are commonly performed in capillary viscometers such as the Ubbelohde-style device shown in Figure 2.6. The polymer solution is drawn up through the capillary and into the upper bulb, and the time required for the solution to flow from the upper etched line to the lower etched line is measured.

In the case of capillary viscometer, it can be shown that:

$$\frac{\eta}{\eta_s} \approx \frac{t}{t_s} \qquad \text{Eqn. 2-17}$$

where t is the flow time required for the polymer solution, and t_s is the flow time required for the pure solvent. The ratio of viscosities in Equation 2-14 can therefore be replaced by a ratio of measured times:

$$[\eta] = \lim_{c \to 0} \frac{\eta_{sp}}{c} = \lim_{c \to 0} \frac{(t/t_s) - 1}{c} \qquad \text{Eqn. 2-18}$$

Determining the intrinsic viscosity thus becomes a matter of performing the flow time measurements on solutions of various polymer concentrations, allowing for an extrapolation to zero concentration (that is, graphically taking the limit as concentration approaches zero). Figure 2.7 is an example of what the results of such a procedure might look like.

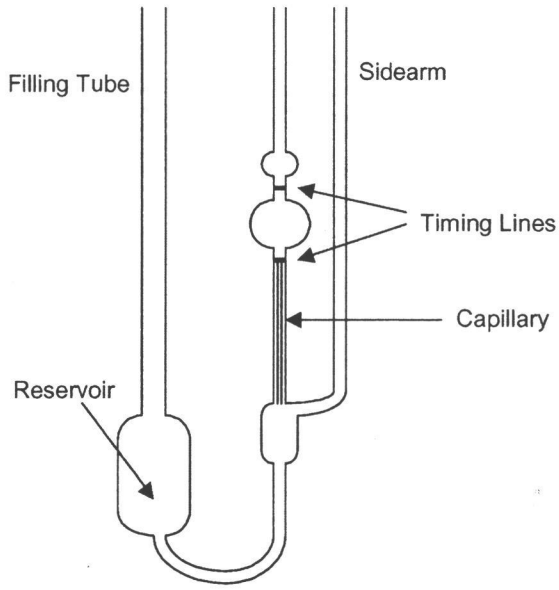

FIGURE 2.6: Schematic of Ubbelohde-style viscometer

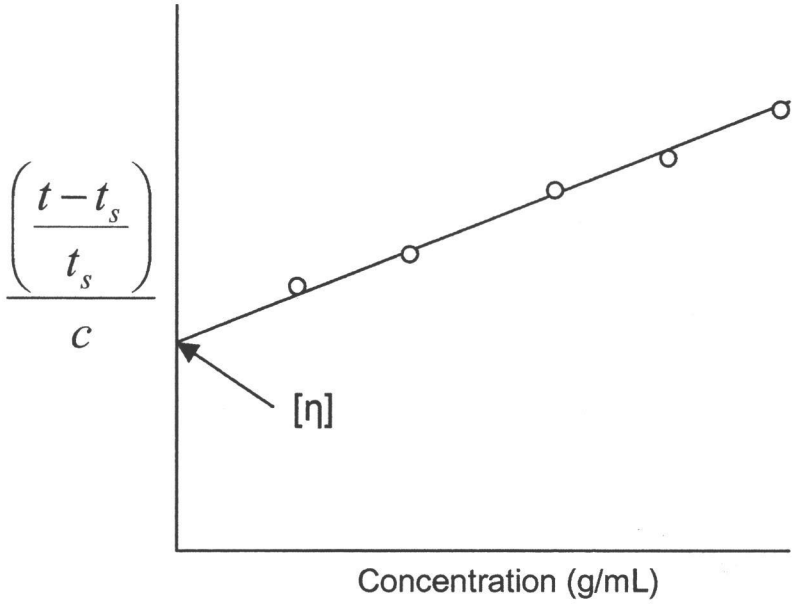

FIGURE 2.7: Example of reduced viscosity plot and determination of intrinsic viscosity

2.3.2.2 Shear Viscosity

Newtonian fluids, such as water, have viscosities that are independent of shear rate. Polymer solutions are typically non-Newtonian, in that their viscosities are a function of shear rate. Determination of this shear rate dependence is vital to the characterization of non-Newtonian fluids, as it has a strong effect on the end use of the product. Solutions that are meant to be injectable through syringes, for example, need to have low viscosities at the high shear rates that they will be subjected to under those conditions.

Rotational viscometers can be used to generate flow curves for polymer solutions. The sample is placed between a fixed plate and a cone that is free to rotate (Figure 2.8). The viscometer drives the cone at a given rate of rotation, and the torque on the cone is measured with an air bearing transducer. The shear stress can then be calculated:

$$\tau = \frac{3T}{2\pi R^3} \qquad \text{Eqn. 2-19}$$

where T is the torque and R is the cone radius.

The shear rate for a cone-and-plate system is given by:

$$\dot{\gamma} = \frac{\varpi r \cos\alpha}{\alpha r} \approx \frac{\varpi}{\alpha} \; for \; small \; \alpha \qquad \text{Eqn. 2-20}$$

where ω is the rotational frequency, α is the cone angle, and r is any given radial position along the cone. From the above, it can be seen that for small cone angles the shear rate is virtually independent of r.

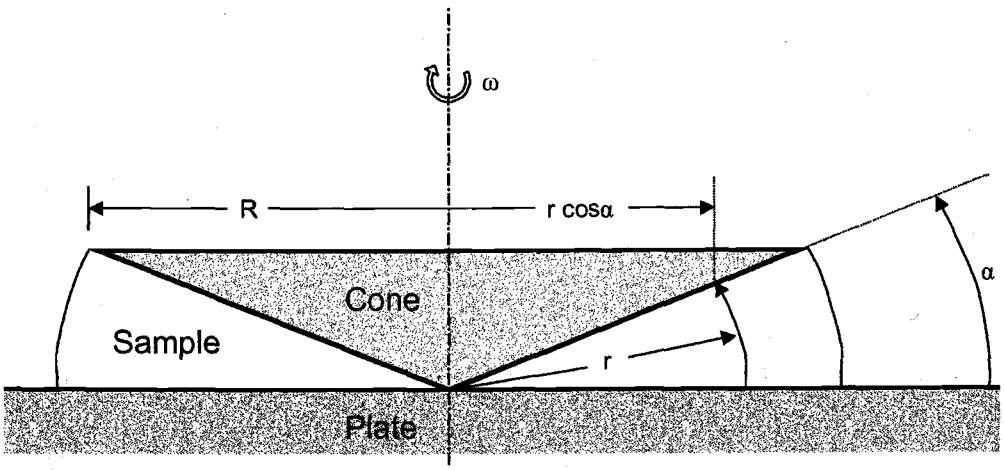

FIGURE 2.8: Schematic of rotational viscometer

Since the definition of viscosity is the ratio of shear stress to shear rate, we are now able to determine viscosity at the measured shear rate. Repeating this for different levels of torque (and therefore different shear rates), a curve of viscosity vs. shear rate can be generated.

2.3.2.3 Dynamic Mechanical Testing

Understanding whether a material stores or dissipates energy upon deformation is critical to determining its appropriate end uses. One way of carrying out this sort of characterization is through dynamic mechanical testing. A sinusoidal strain is applied to the material in question, where the strain is given by:

$$\gamma = \gamma^{'} \sin(\omega t) \qquad \text{Eqn. 2-21}$$

When an ideal Hookean solid—the classical mechanical model of which is a spring—is subjected to a sinusoidal shear deformation, the applied strain results in a stress proportional to the strain:

$$\tau = G\gamma = G\gamma^{'} \sin(\omega t) \qquad \text{Eqn. 2-22}$$

It is obvious that the generated stress is exactly in phase with the applied strain. In this case, energy applied toward deformation is stored in the material.

On the other hand, when an ideal Newtonian fluid is subjected to a sinusoidal shear deformation, the generated stress is proportional, not to the strain, but to the rate of strain:

$$\tau = \eta \dot{\gamma} = \eta \omega \gamma' \cos(\omega t) \qquad \text{Eqn. 2-23}$$

In this case the applied strain and the generated stress are exactly out of phase (the stress is greatest at the midpoint of the cycle, and is zero at the extremes). In this case, energy applied toward deformation is dissipated and lost. The classical mechanical model of this situation is the dashpot.

A real polysaccharide system will exhibit some intermediate response between the ideal Hookean solid and the ideal Newtonian fluid (and hence is not termed elastic or viscous, but rather viscoelastic). The degree of solid-like and liquid-like behavior that a given viscoelastic system exhibits can be quantified by applying a strain to the material and resolving the resulting stress into in-phase and out-of-phase components. The storage modulus can then be defined:

$$G' \equiv \frac{\tau'}{\gamma'} \qquad \text{Eqn. 2-24}$$

where τ' is the in-phase component of stress and γ' is the in-phase component of strain. (Note that the out-of-phase component of strain is zero.)

Likewise, the loss modulus can be defined:

$$G'' \equiv \frac{\tau''}{\gamma'} \qquad \text{Eqn. 2-25}$$

where τ'' is the out-of-phase component of stress. The storage modulus is a measure of solid-like, or elastic, character. The loss modulus is a measure of liquid-like, or viscous, character.

Whether a material exhibits primarily elastic or primarily viscous behavior may depend, in part, upon the frequency and magnitude of the imposed strain. Polymeric materials exhibit a characteristic relaxation time, τ_R, which describes the ability of the polymer chains to disentangle and flow past one another and which is proportional to the polymer molecular weight to the 3.4 power.

$$\tau_R \propto M^{3.4} \qquad \text{Eqn. 2-26}$$

If a polymeric material is deformed on a time scale shorter than its relaxation time then the polymer chains are unable to disengage and the material is prone to elastic

behavior. If the material is deformed over a longer time scale, the polymer is able to relax and will tend to exhibit viscous behavior. If G' remains higher than G" at all frequencies, the sample may be classified as a gel or as a rubber-like material (Figure 2.9). In some samples, G' is smaller than G" at low frequencies but overtakes G" at higher frequencies; the point at which this occurs is termed the crossover frequency, ω_c (Figure 2.10).

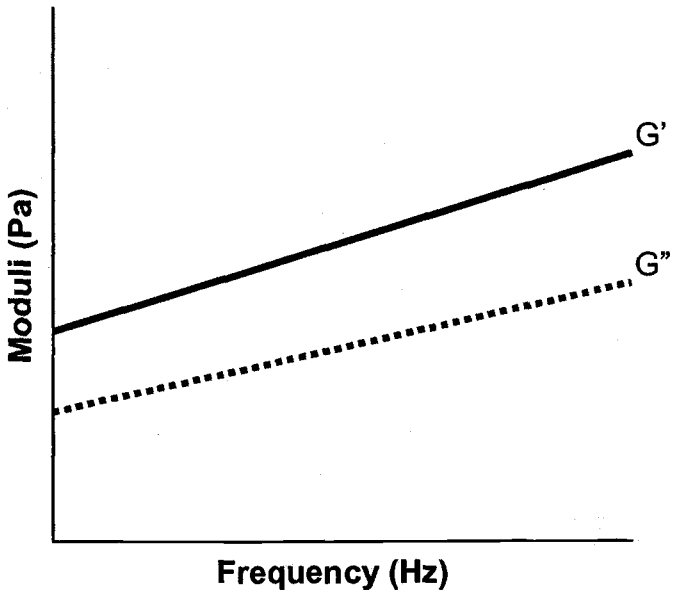

FIGURE 2.9: Example of dynamic mechanical testing data for gel-like material

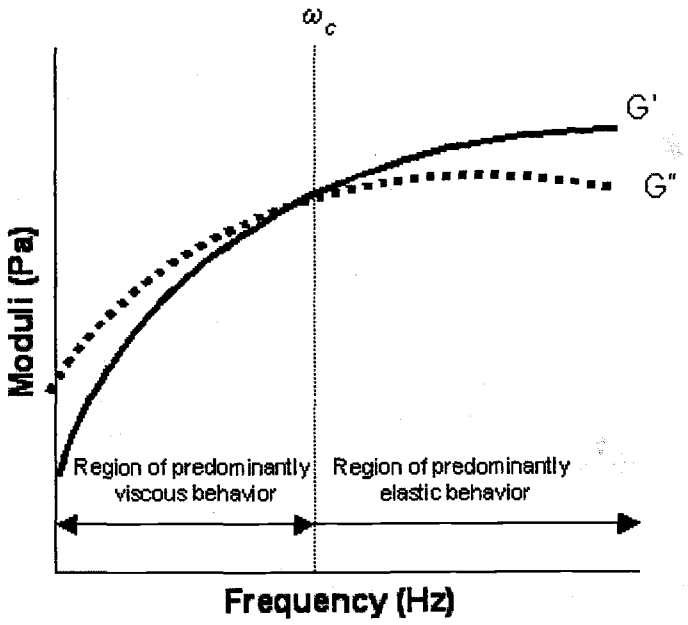

FIGURE 2.10: Example of dynamic mechanical testing data for material with cross-over frequency

There is a theoretical relationship between the cross-over frequency and the relaxation time, given by:

$$\tau_R \propto (\omega_c)^{-1} \qquad \text{Eqn. 2-27}$$

Combining Equations 2-25 and 2-26, we find:

$$\tau_R \propto (\omega_c)^{-1} \propto M^{3.4} \qquad \text{Eqn. 2-28}$$

It is clear that materials which exhibit a lower cross-over frequency will also exhibit a longer relaxation time, and must therefore have a larger molecular weight. Dynamic oscillatory testing data is thus provides additional information on the relative molecular weights of similar materials.

2.4 METHODS AND MATERIALS

2.4.1 Materials Used

Three samples of hyaluronic acid were donated by Biozyme Laboratories. The samples were of differing molecular weights but were all extracted from the same source—rooster comb—and are hereafter identified by the codes HAC3Na, HAC2Na, and HAC1Na. Biozyme Laboratories indicates that HAC3Na should have the highest molecular weight, and HAC1Na should have the lowest, based upon measurements of intrinsic viscosity.

Two solvents were used in the characterization of hyaluronic acid: a phosphate buffered saline (PBS) and a solvent for light scattering. The PBS is meant to mimic human synovial fluid, and so has a comparable pH, ionic strength, and osmolality. Its composition is 7.813 mM sodium phosphate dibasic, 21.875 mM sodium phosphate monobasic, and 150 mM sodium chloride in distilled water.

The light scattering solvent is composed of 0.5wt% sodium azide and 0.1 M sodium nitrate in de-ionized water.

2.4.2 Intrinsic Viscosity

Stock solutions of hyaluronic acid (HAC3Na, HAC2Na, HAC1Na) in PBS were made at 1000 ppm. Subsequent dilutions of stock with PBS resulted in further concentrations of 800 ppm, 600 ppm, 400 ppm, and 200 ppm. The time measurements were carried out at room temperature with an Ubbelohde-style capillary viscometer.

2.4.3 Light Scattering

For each grade of hyaluronic acid, a stock solution was made at a concentration significantly lower than its C^*—light scattering measurements become highly inaccurate when polymer molecules begin to interact and entangle. To help eliminate the deleterious effect of dust particles upon light scattering, the sodium nitrate solvent was pre-filtered through a 0.1 micron syringe filter before use. The solution was then prepared by weighing the solvent and solute on an analytical balance accurate to 0.1 milligram, and was stirred overnight at room temperature. Dilution of the stock solution into clean scintillation vials then resulted in final samples of 16.7%, 33.3%, 50.0%, 66.7%, 83.3%, and 100% of the stock concentration. These samples were filtered again through 10 micron syringe filters,

and the vials were soaked in 20% nitric acid overnight in order to remove deposits from the glass. The samples were then ready for experimental use.

A Wyatt DAWN low-angle laser light scattering instrument, operated in batch mode with a laser wavelength of 690 nm, was used for all light scattering measurements.

2.4.4 Rheological Characterization

Solutions were prepared in PBS and stirred overnight at room temperature. All measurements were taken with a Bohlin CS 50 Controlled Stress Rheometer. Unless otherwise noted, measurements were taken at 37° C with a cone-and-plate geometry, using a 4° cone with a 40mm diameter. Dynamic mechanical data was gathered at frequencies from 0.1 Hz to 10 Hz, and at strains of 10% and 25%. Constant rate data was gathered at shear rates from approximately 0.1 to 1000 s^{-1}.

2.5 RESULTS AND DISCUSSION

2.5.1 Light Scattering

Results as generated by the Wyatt Corporation software are given below as Figures 2.11, 2.12, 2.13, and tabulated in Table 2.1.

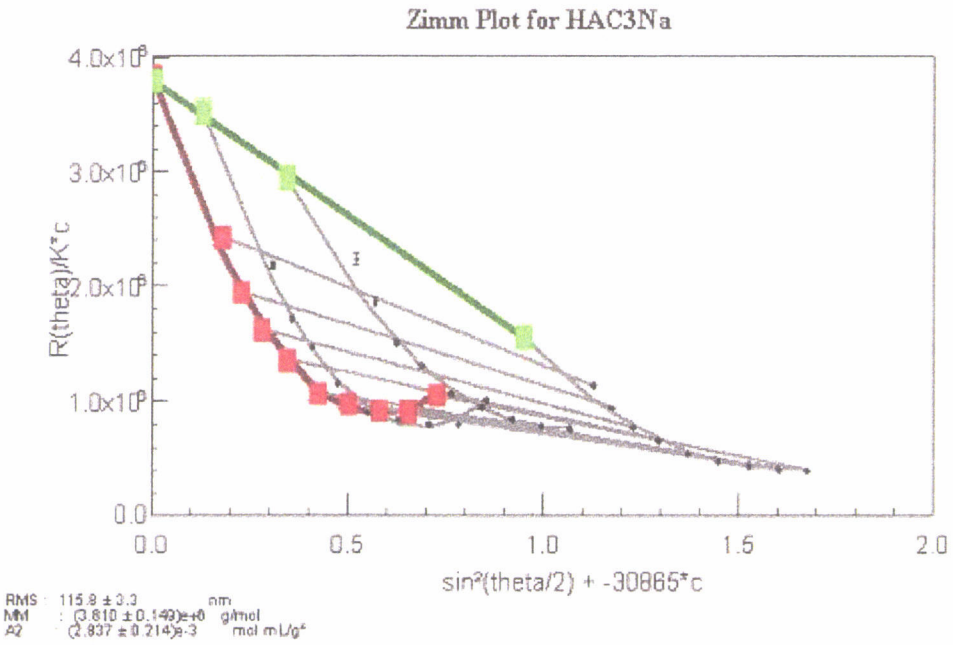

FIGURE 2.11: Light scattering results for HAC3Na

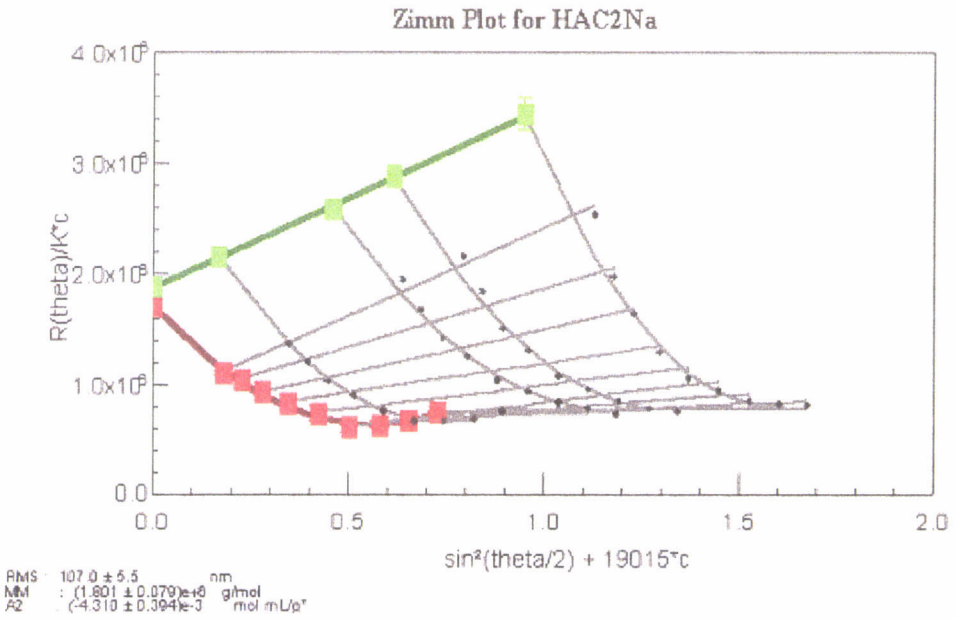

FIGURE 2.12: Light scattering results for HAC2Na

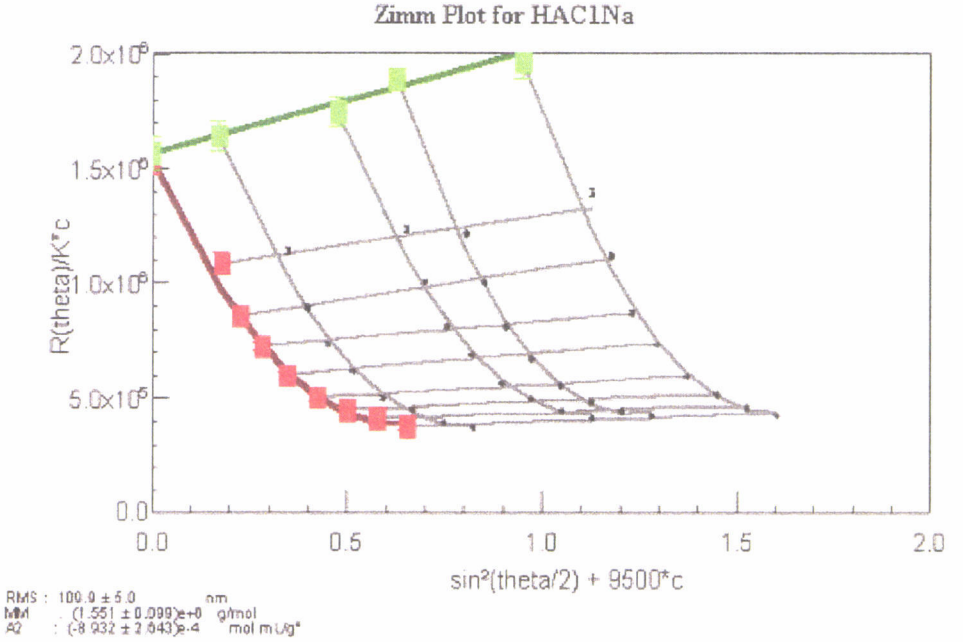

FIGURE 2.13: Light scattering results for HAC1Na

	M_w (x10^6) (Da)	r_g (nm)
HAC3Na	3.810 ± 0.149	115.8 ± 3.3
HAC2Na	1.801 ± 0.079	107.0 ± 5.5
HAC1Na	1.551 ± 0.099	109.9 ± 5.0

TABLE 2.1: Results of light scattering measurements

These results indicate that the sample of hyaluronic acid designated HAC3Na has the highest molecular weight as well as the largest root-mean-square radius, followed by HAC2Na and HAC1Na. All HA samples have similar root-mean-square radii; the measured values are within one another's margin of error, and so a firm ranking is not possible with the data at hand (although it does appear likely that HAC3Na has a larger root-mean-square radius that the other two samples).

2.5.2 Intrinsic Viscosity

Results of the intrinsic viscosity measurements are reproduced in Table 2.2, along with calculated values for C^*. Values of k' are also calculated in accordance with the Huggins equation for dilute polymer solutions:

$$\frac{\eta_{sp}}{c} = [\eta] + k'[\eta]^2 c \qquad \text{Eqn. 2-29}$$

Typically, k' is close to 0.4 for most polymer-solvent systems. In general, having the value of k' for a polymer-solvent system is useful in that, if the intrinsic viscosity is also known, it allows for estimation of dilute solution viscosity vs. concentration.

From Table 2.2, it can be seen that the highest intrinsic viscosity is possessed by HAC3Na, followed by HAC2Na and HAC1Na. This is in keeping with the results from light scattering, which indicated that HAC3Na has the highest molecular weight and would therefore most likely exhibit the highest intrinsic viscosity.

	k'	[η] (mL/g)	C^* (mg/mL)
HAC3Na	0.577	2631	0.38
HAC2Na	0.314	1303	0.77
HAC1Na	0.267	1015	0.98

TABLE 2.2: Results of intrinsic viscosity measurements

Because the overlap concentration, C^*, is the reciprocal of intrinsic viscosity, solutions of HAC3Na leave the dilute regime at lower solute concentrations than do either HAC2Na or HAC1Na, and solutions of HAC2Na leave the dilute regime at a lower solute concentration than does HAC1Na.

Having both molecular weight (via light scattering) and intrinsic viscosity measurements, one can obtain the parameters in the Mark-Houwink-Sakurada equation (Eqn. 2-15). Figure 2.14 is a plot of the intrinsic viscosity of each HA sample versus the measured molecular weight. Using this data, an iterative numerical method was employed to minimize the error which results when the MHS equation is used to predict intrinsic viscosity. The parameter K was calculated to be $1.69*10^{-3}$ and the parameter a was calculated to be 0.94, resulting in the following MHS equation for HA in PBS:

$$[\eta] = 1.69*10^{-3}M^{0.94} \qquad \text{Eqn. 2-30}$$

Compare to the MHS equation which has been determined for xanthan gum in saline solution (Lecoutier and Chauveteau, 1984):

$$[\eta] = 6.3*10^{-3}M^{0.93} \qquad \text{Eqn. 2-31}$$

The parameter *a* takes on values from 0.6 to 0.8 for random coil polymers, and values of approximately 1.0 for semi-rigid polymers such as xanthan gum. This result is therefore a good indication that hyaluronic acid behaves as a semi-rigid polymer in PBS.

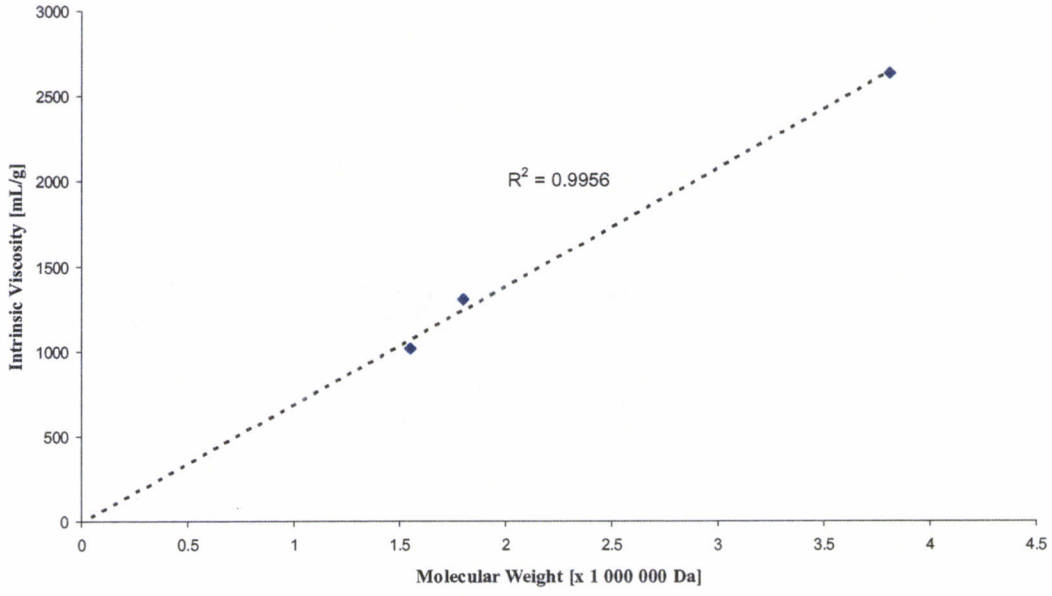

FIGURE 2.14: Correlation between molecular weight and intrinsic viscosity for samples of HA in PBS

2.5.3 Rheological Characterization

Dynamic oscillatory shear (Figure 2.15) and constant shear rate (Figure 2.16) data for the three grades of hyaluronic acid, at concentrations of 1.0wt% in PBS at 37°C, are presented below.

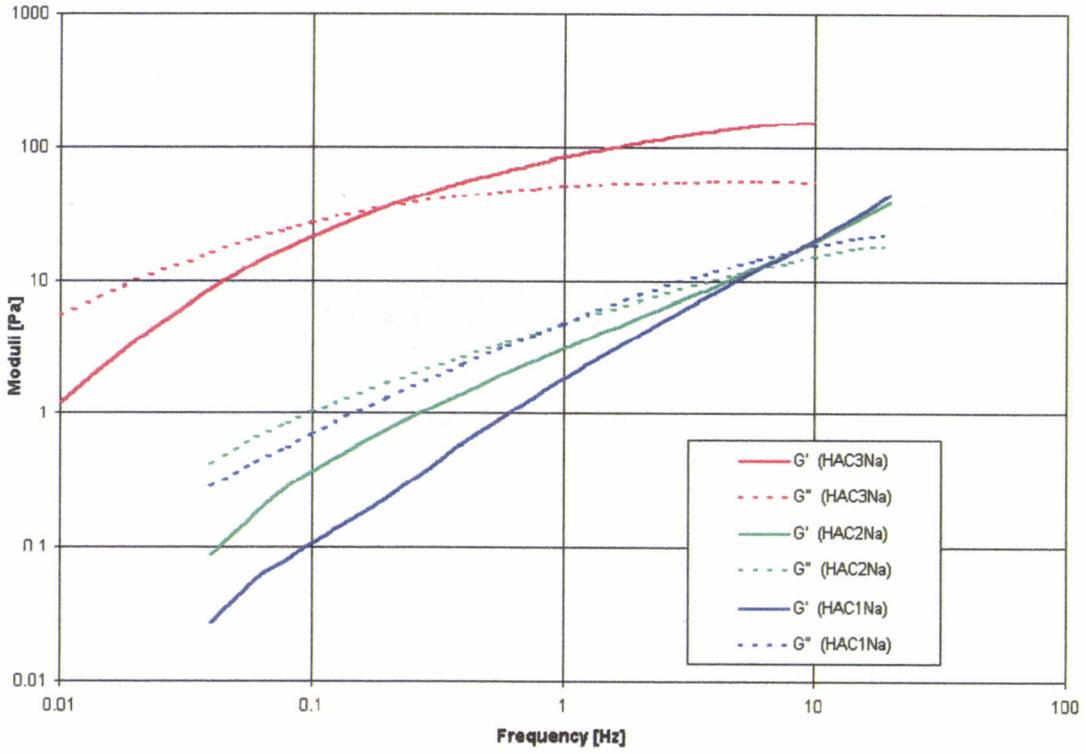

FIGURE 2.15: Dynamic mechanical testing data for 1.0 wt% hyaluronic acid in PBS, with strain = 0.25, T = 37° C

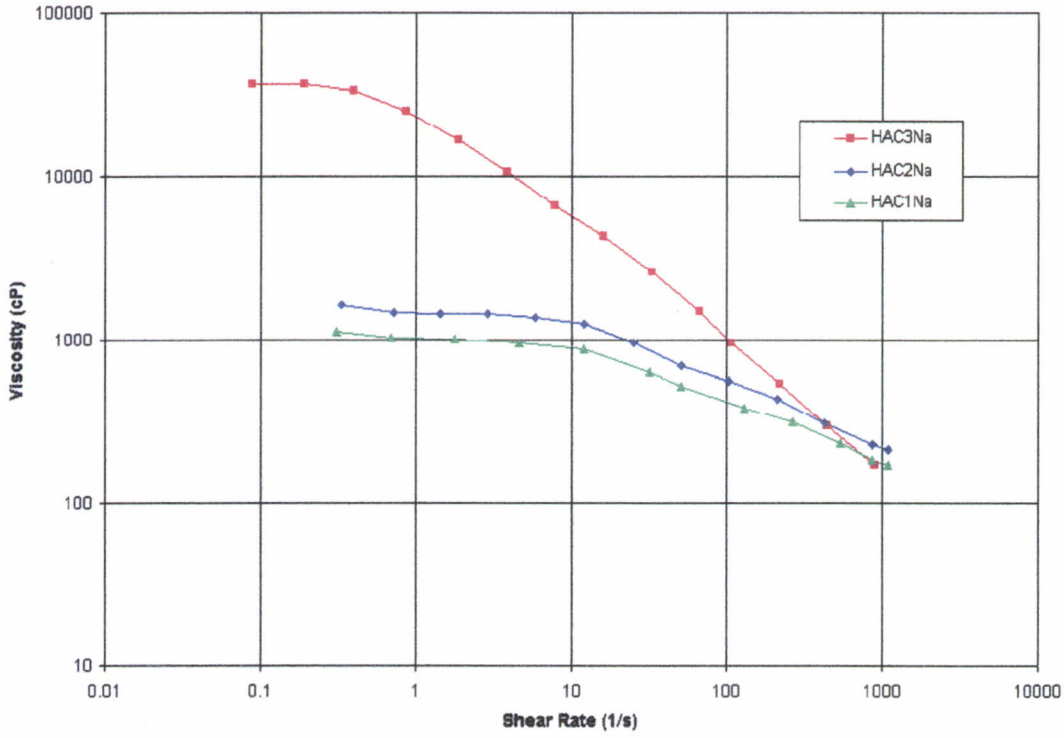

FIGURE 2.16: Constant rate data for 1.0wt% hyaluronic acid solutions in PBS at 37° C

In Figure 2.15, the crossover frequency for HAC3Na is lower than that of either HAC2Na or HAC1Na, and the crossover frequency for HAC2Na is lower than that of HAC1Na. Referring back to Equation 2-28, this provides more evidence, along with the light scattering and intrinsic viscosity measurements, that HAC3Na has the highest molecular weight and HAC1Na the lowest.

The constant shear rate data (Figure 2.16) reveals that all three HA samples exhibit similar shear-thinning behavior, with a "plateau region" of fairly constant viscosity

over a range of low shear rates, followed by a viscosity drop at higher shear rates. The magnitude of the plateau regions (known as the zero-shear viscosity) follows the molecular weight of the samples, with HAC3Na having the highest viscosity and HAC1Na having the lowest. Notice however that the zero-shear viscosity does not scale linearly with molecular weight. This is due to the introduction of entanglement effects; since the HA solutions were all the same weight percent, the solutions containing higher molecular weight HA will exhibit more entanglement and therefore a higher viscosity. The zero-shear viscosity of concentrated polymer solutions is typically proportional to the 3.4 power of molecular weight, though, as noted in the literature review, Fouissac et al. (1993) report a fourth power dependence for HA solutions. From the zero-shear viscosity data in Figure 2.15 and the molecular weight data in Table 2.1, the author confirms that the zero-shear viscosities of concentrated HA solutions are proportional to approximately the fourth power of molecular weight (Figure 2.17).

In summary: the molecular weights of three discrete HA samples have been measured through multi-angle laser light scattering, their intrinsic viscosities measured through dilute solution viscometry, and their rheological behavior in solution has been characterized through constant shear rate and dynamic oscillatory shear rheometry techniques. The Huggins parameter k' has been calculated for

each molecular weight of HA considered, and the Mark-Houwink-Sakurada parameters have been determined for the HA-PBS system.

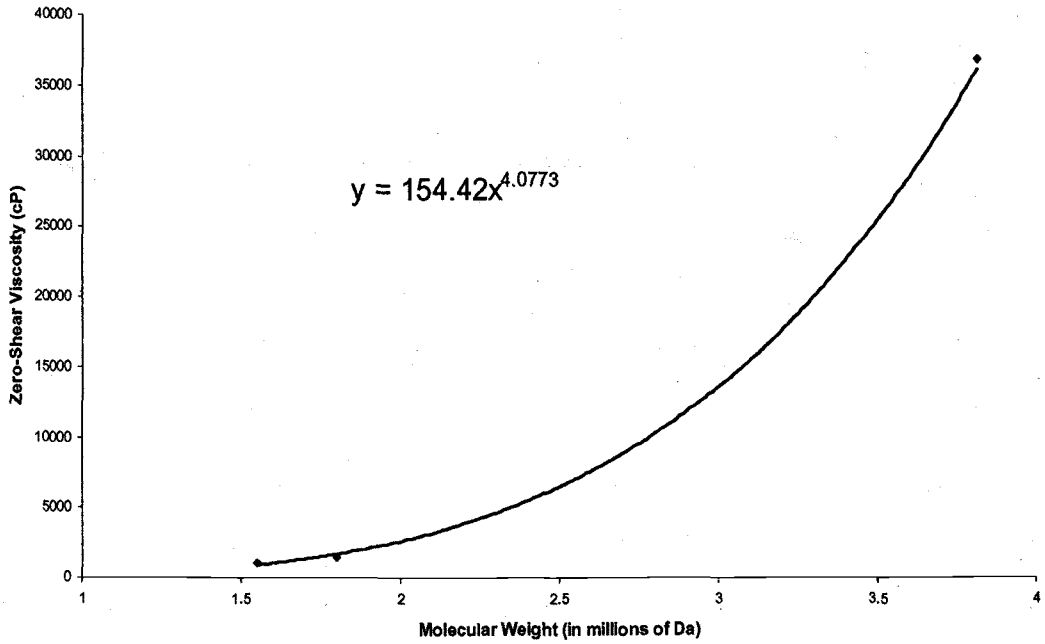

FIGURE 2.17: Zero-shear viscosity of HA in PBS as a function of HA molecular weight

3. HYALURONIC ACID AND FIBRIN CLOTTING

3.1 INTRODUCTION

The study of possible interactions between hyaluronan and fibrinogen during the fibrin clotting process is very likely to be of more than academic interest. Certain pieces of circumstantial evidence (see below) suggest that hyaluronan has an important role to play in blood clotting—whether this role is that of a pro-coagulant or that of a clotting regulator remains hazy. If either case proves true, hyaluronan-containing products could conceivably find medical use as anti- or pro-coagulants.

Several studies have been performed to date in an attempt to elucidate the hyaluronan-fibrin relationship. LeBoeuf et al. have been pioneers in this field of study: in 1986 the group studied whether a specific interaction occurs between the macromolecules; in 1987 they used spectrophotometry to monitor clotting rates of fibrin with and without hyaluronan incubated with the sample. Questions remain, however, as to the validity of this experimental procedure, as will be discussed below.

This research attempts a more thorough study of hyaluronic acid and fibrin clotting. Solutions of fibrinogen were incubated with hyaluronic acid before introducing the thrombin enzyme, and the progress of the clot formation was monitored via a

continuous measurement of the elastic modulus of the sample. This rheological approach to monitoring hyaluronic acid and fibrin clot formation is relatively novel. The use of spectrophotometry has been more common, but brings into question the possibility of excluded volume effects producing artificially high levels of light absorption. Such measurements would indicate a fast rate of clotting regardless of whether or not the clot was, in *macro*, actually colluding into a solid structure.

Monitoring a clot's elastic modulus, on the other hand, necessarily gives a true measure of the macroscopic behavior of the sample, but does not yield direct information regarding the molecular mechanisms involved. Furthermore, by performing the experiments with a range of HAs with different, known molecular weights and intrinsic viscosities, it becomes possible to relate an observed affect on clotting to molecular size and degree of networking—a issue which has thus far been neglected in the literature.

3.2 LITERATURE REVIEW

The polymerization of fibrin is a key step in the process of wound healing (Campbell, 1996). The formation of this clot is the end result of a complex cascade of biological reactions, the penultimate step of which is the thrombin-catalyzed cleavage of the fibrinogen protein (Nemerson & Furie, 1980). Fibrinogen is a large

molecule (450Å in length, molecular weight of 340 000) composed of three polypeptide chains, two of which tend to release from the complex in the presence of thrombin (Doolittle, 1984; Bettelheim & Bailey, 1952); the resulting structure is known as fibrin, and is capable of linear and lateral aggregation with other fibrin molecules.

Researchers have long suspected that hyaluronic acid (HA) may have an important role in the aggregation of fibrin, making it a major player in wound healing. The evidence has been circumstantial: HA is found only in low concentrations in plasma (Engstrom-Laurent et al., 1985), but at the site of a recent wound its concentration increases drastically (Bentley, 1968). It has also been found that the liver actively removes HA from the blood (Fraser et al., 1984), which may indicate that high concentrations of HA in blood represents a dangerous condition to the organism; it has been theorized that the liver must regulate blood HA levels in order to prevent uncontrolled fibrinogen-HA bindings within the vessels, which could possibly result in increased blood viscosity (Weigel et al., 1986).

LeBoeuf et al. (1986) injected various proteins through an affinity chromatography matrix prepared through the coupling of HA to Sepharose. Approximately 60% of the fibrinogen input was bound, a quantity 4-50 times greater than the binding observed for ovalbumin, orosomucoid, DNAse I, haptoglobin, or lysozome. The

possibility of nonspecific interactions between fibrinogen and Sepharose was addressed through the use of an ethanolamine-Sepharose control matrix; the control matrix bound only 12-17% of the quantity of fibrinogen that the HA-Sepharose matrix was able to bind. The possibility of nonspecific electrostatic binding of fibrinogen to HA-Sepharose was addressed by varying the ionic strength; the binding was stable at high ionic strength, and only 18-27% of bound fibrinogen was released at low ionic strengths (0.05 M NaCl). (The last figure is of questionable value in this discussion, considering that the solubility of fibrinogen is drastically reduced at low ionic strength [Mosesson & Sherry, 1966]—the fibrinogen may simply have precipitated out of solution.) Nonspecific interactions were thus ruled out, indicating that fibrinogen binds hyaluronic acid with a good degree of specificity. This is a situation that, in biological systems, often indicates physiological significance.

To ascertain whether HA had an affect on the aggregation of fibrin, LeBoeuf et al. (1987) measured the rate of fibrin clotting both with and without HA present. The measurement was performed indirectly, by noting the capacity of the solution to absorb light at 450nm; since prior work has positively correlated the turbidity of fibrin gels to the mass:length ratio of fibrin fibrils (Carr et al., 1977; Shah et al., 1982), this method is justified. The results of the spectrophotometry experiments indicate that the absorbance (A_{450}) increases as the fibrin clotting progresses,

eventually reaching some steady state value, and that both the rate of increase and the steady state value are much greater when HA is present. A_{450} increased up to 15 times faster when in the presence of HA, and its final value was up to 8 times greater.

Hayen et al. (1999), in the course of their studies on the influence that HA may exert upon tumor cell migration through fibrin gels, report that confocal laser microscopy reveals drastic structural differences in fibrin gels polymerized in the absence of HA and those polymerized in its presence. The former gels "consisted of fine fibers and very small pores" while the later displayed "large pores and significantly thickened fibrin fibers."

Between these results and the earlier work of LeBoeuf et al., it is thus well established that HA affects the polymerization of fibrin. The question that remains is whether the interaction is a specific one. If it is not, then the phenomenon is likely to be of little physiological significance—a novelty only encountered *in vitro*.

LeBoeuf et al. (1989) recognized the possibility that nonspecific exclusion effects were responsible for the observed changes in the behavior of fibrin clotting. If compartmentalization were to occur, then the increased concentration of fibrinogen

found in the resulting "pockets" might change the kinetics of aggregation. In disregarding this possibility, the LeBoeuf team notes that the HA fragments used in the experiment were relatively small ones (Mr = 30 - 40 kDa) and therefore unlikely to cause compartmentalization, and that "other anionic polysaccharides such as polygalacturonic acid... did not work." The last comment is in reference to the notion that if exclusion effects were at work, then most large anionic polysaccharides (of which HA is an example) would lead to results similar to those observed with HA.

In a further attempt to address this concern, fibrinogen and thrombin were incubated with dextran rather than HA (Weigel et al., 1989). Dextran, a polysaccharide, has been shown to exhibit exclusion effects in solution (Comper & Laurent, 1978). The dextran-containing solution did not exhibit behavior significantly different from the control solution, however, leading the authors to conclude that nonspecific exclusion effects were not responsible for the HA-induced acceleration in fibrin clotting. It should be taken into consideration, however, that these observations are in conflict with the results reported by Carr and Gabriel (1980), who noted a substantial acceleration in fibrin polymerization when in the presence of dextran. These two conclusions cannot be easily reconciled; it may be of some import that Carr and Gabriel used a much higher molecular weight dextran than did Weigel et al. (1989)—70 000 versus 40 000.

Carr and Gabriel may be observing exclusion effects that LeBoeuf's team were not able to achieve with a lower molecular weight polysaccharide.

Larsen (1998) approaches the HA/fibrinogen relationship from another angle: as the fibrin in a solution undergoes aggregation, the elastic modulus (G') of said solution increases correspondingly. If HA acts as a procoagulant with respect to fibrin clot formation, a greater rate of increase in G' and/or a higher final value of G' would be expected for a solution of fibrinogen, thrombin and HA as compared to a control solution of fibrinogen and thrombin alone. Larsen (1998) reports results contrary to this expectation, citing this as evidence that HA, rather than acting as a procoagulant, instead acts to interfere with normal clot formation. Unfortunately, Larsen did not utilize natural HA in her experiments, but rather used a crosslinked derivative of hyaluronan (a *hylan*). Hylan may interfere with fibrin clot formation, but since crosslinking a polymer often results in drastic changes in the molecule's physical properties and interactions, one cannot draw firm conclusions from this study regarding the role of natural HA in the clotting process.

Larsen (1998) repeats the spectrophotometry experiments of LeBoeuf et al. (1987), albeit using a hylan instead of natural hyaluronan, and reports comparable results—a greater rate of increase in A_{450} and a higher final A_{450}. It is also reported that similar results can be obtained by replacing HA in the experiment with other high-

molecular-weight polymers; Larsen uses DNA as an example. This is cited as evidence that the affect HA has on A_{450} is due to excluded volume effects alone, and Larsen concludes that HA has no role in the fibrin clotting process as it occurs *in vivo*. The possibility exists, however, that HA's effect on A_{450} is due to a specific interaction with fibrinogen, while DNA's effect on A_{450} can be ascribed to excluded volume effects alone.

3.3 EXPERIMENTAL BACKGROUND AND THEORY

Dynamic oscillatory shear testing, as described in Chapter 2, can be used to follow the formation of clots by monitoring the elastic modulus over time. In this situation, it is not desirable to perform measurements at a variety of frequencies, since it is not the frequency dependence of the moduli which is of interest. Rather, the test is performed continuously at a single frequency over time. As the material clots, the elastic modulus (G') will increase at a greater rate than will the viscous modulus (G"). The time at which G' exceeds G" is a convenient measure of clotting time. Note that this is somewhat equivalent to the crossover point in dynamic oscillatory shear testing, though in this case the crossover occurs at a certain *time* rather than a certain *frequency*.

3.4 METHODS AND MATERIALS

Fibrinogen and thrombin were supplied by Harimex, Inc. (Toronto, Canada) under the tradename Fibrimex®, and were used as received with no modifications. The fibrinogen and thrombin were stored at -15° C, and were thawed in a water bath at room temperature for 30-45 minutes prior to use. A Bohlin CS 50 Controlled Stress Rheometer was used to take the measurements, with a constant oscillation of 1 Hz and a shear stress of 5 Pa. All tests were performed at 37° C.

The results of four experimental sessions are reported below. A control, consisting of 0.1 mL of thrombin solution added to 2.0 mL of fibrinogen solution, was performed at the start and the end of each session. During two sessions, 1.55 mg/mL of HA was added to the fibrinogen. During the other two sessions, enough HA was added to the fibrinogen to reach a C/C^* ratio of either 3 or 0.5. (See Table 3.1. Values for C^* were obtained as described in Chapter 2.) The rationale for this will shortly become evident.

	C = 1.55 mg/mL		C/C* = 3		C/C* = 0.5	
	C*	C/C*	C*	C	C*	C
HAC3Na	0.38	4.08	0.38	1.14	0.38	0.19
HAC2Na	0.75	2.07	0.75	2.25	0.75	0.38
HAC1Na	0.98	1.58	0.98	2.94	0.98	0.49

TABLE 3.1: Concentrations used for clotting experiments

3.5 RESULTS AND DISCUSSION

Original results from all clotting experiments are reproduced below.

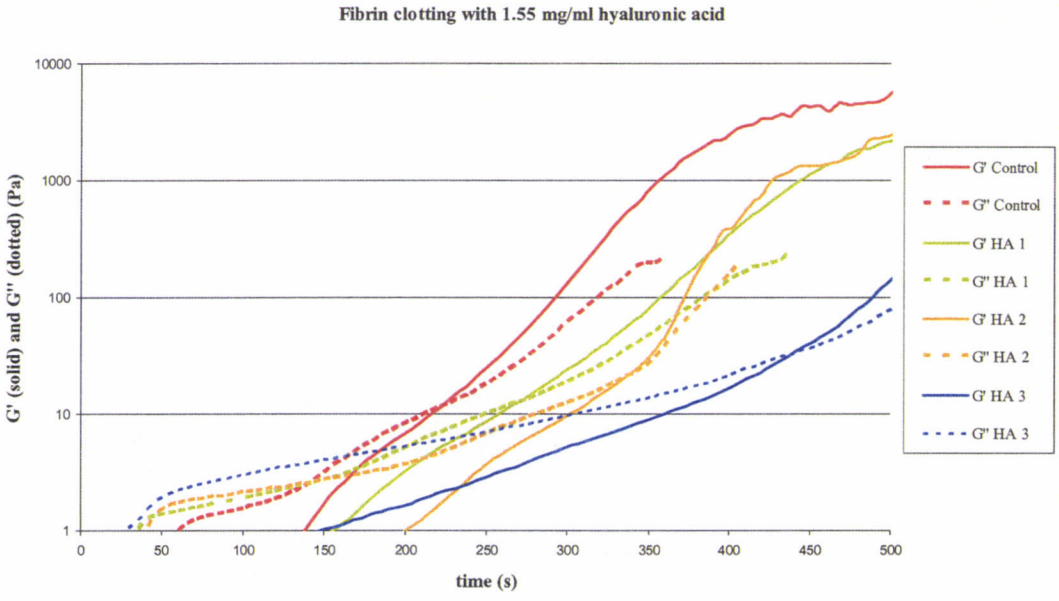

FIGURE 3.1: Clotting results with 1.55 mg/ml of hyaluronic acid added to 2 ml fibrinogen + 0.1 ml of thrombin (first run)

SAMPLE	CLOTTING TIME (seconds)
Control	222
HA 1	270
HA 2	336
HA 3	438

TABLE 3.2: Clotting times associated with Figure 3.1

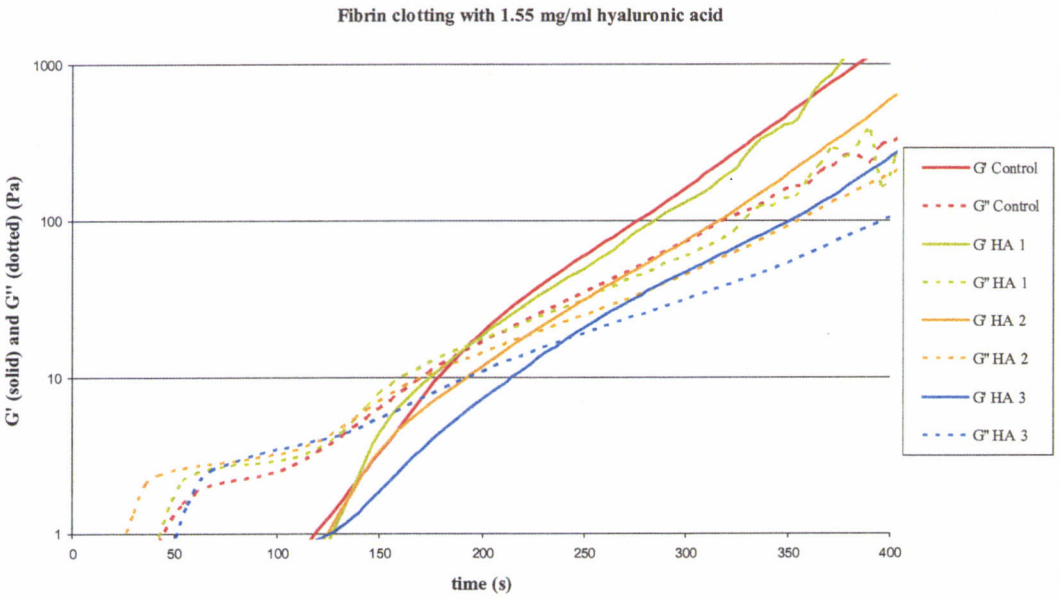

FIGURE 3.2: Clotting results with 1.55 mg/ml of hyaluronic acid added to 2 ml fibrinogen + 0.1 ml of thrombin (second run)

SAMPLE	CLOTTING TIME (seconds)
Control	190
HA 1	198
HA 2	222
HA 3	242

TABLE 3.3: Clotting times associated with Figure 3.2

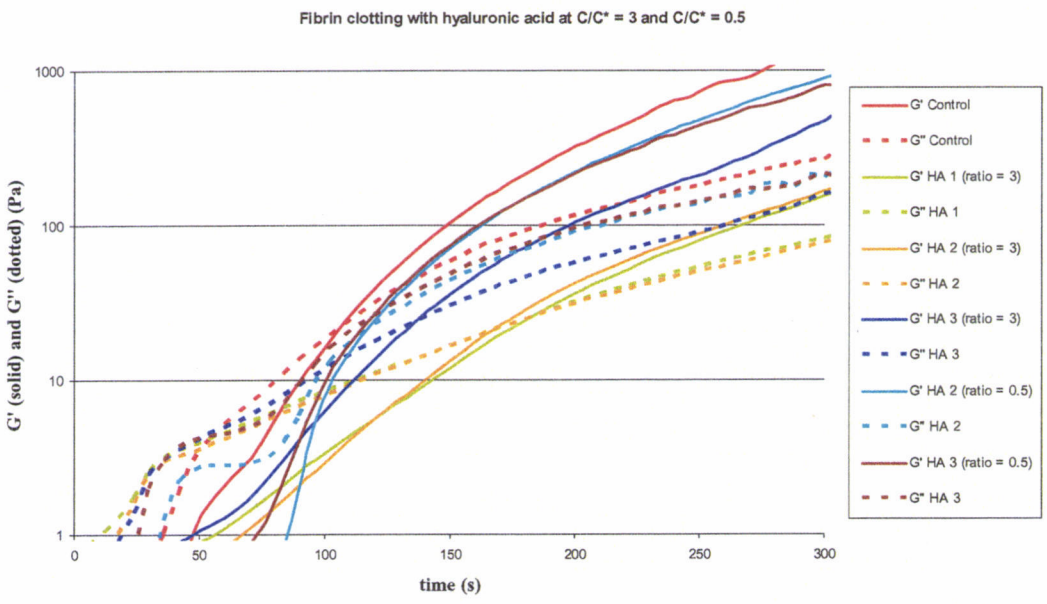

FIGURE 3.3: Clotting results with an HA concentration ratio (C/C^*) of 3.0 and 0.5 added to 2 ml fibrinogen + 0.1 ml of thrombin (first run)

SAMPLE	CLOTTING TIME (seconds)
Control	108
HA 1 (C/C* = 3)	180
HA 2 (C/C* = 3)	168
HA 3(C/C* = 3)	138
HA 2 (C/C* = 0.5)	120
HA 3 (C/C* = 0.5)	120

TABLE 3.4: Clotting times associated with Figure 3.3

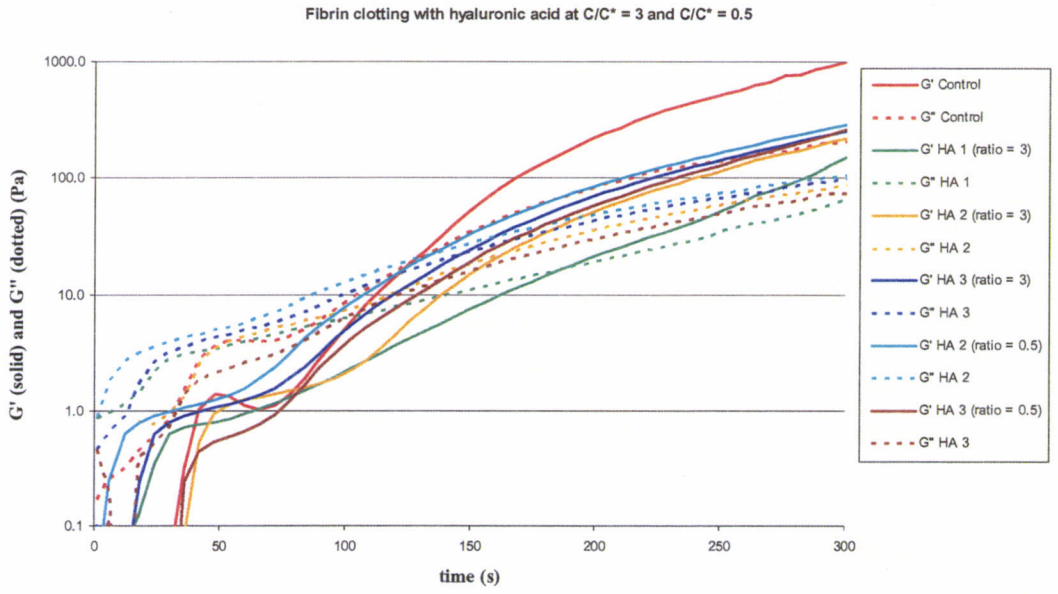

FIGURE 3.4: Clotting results with an HA concentration ratio (C/C^*) of 3.0 and 0.5 added to 2 ml fibrinogen + 0.1 ml of thrombin (second run)

SAMPLE	CLOTTING TIME (seconds)
Control	126
HA 1 (C/C* = 3)	192
HA 2 (C/C* = 3)	168
HA 3(C/C* = 3)	150
HA 2 (C/C* = 0.5)	140
HA 3 (C/C* = 0.5)	134

TABLE 3.5: Clotting times associated with Figure 3.4

In all cases, hyaluronic acid appeared to act as an anti-coagulant, slowing down the clotting processes and weakening the final formed clot. When an identical concentration of hyaluronic acid was used in each experiment (1.55 mg/mL), it can be seen that HA of higher molecular weight retarded the clotting more and resulted in lower plateau values of G'. On the other hand, when an identical C/C^* ratio was used in each experiment, it appears that HA of lower molecular weight retarded the clotting more and resulted in lower plateau values of G'. In order to address this apparent discrepancy, the following theory is proposed:

Hyaluronic acid acts as an anti-coagulant through two complementary mechanisms. The specific binding between HA and fibrinogen, described by LeBoeuf and colleagues, acts to retard fibrin clotting through steric hindrance. In addition, HA forms a network in solution which retards fibrin clotting by hindering free diffusion of fibrin and thrombin and by preventing isolated regions of fibrinogen from linking from and strengthening the clot in *macro*.

The experimental results provide evidence for this theory. When roughly identical concentrations of HA were used, the number of repeat units of HA in each experimental solution were also roughly identical. That is, while 1.55 mg/mL of HAC3Na represents fewer molecules than does 1.55 mg/mL of HAC1Na, the number of HA repeat units are very similar. In this event the specific binding

effect, if indeed present, would have had a similar effect on clotting in each experiment; the degree of networking would be the factor to differentiate the solutions. This is exactly what was noted: HAC3Na is more networked at 1.55 mg/mL than is either HAC2Na and HAC1Na, owing to its lower C^*, and HAC3Na retards the clotting the most.

When the same C/C^* was used in each experiment, it should be expected that the degree of networking present in each solution should be roughly equivalent. The concentration required to reach that particular ratio differs for each HA sample, however, meaning that a solution of HAC3Na with a $C/C^* = 3$ has fewer repeat units than a solution of HAC2Na or HAC1Na with a $C/C^* = 3$. Since the degree of networking is similar, it will be the specific binding effect, if present, that will now differentiate the solutions. Again, this is what was noted: HAC1Na, having more repeat units in solution than HAC3Na or HAC2Na, retarded clotting the most. HAC3Na, with the fewest number of repeat units in solution, retarded clotting the least. As further evidence of a specific binding effect, note that solutions with an HA $C/C^* = 0.5$ also exhibited slower clotting times than the control, although at this ratio there should be no network exclusion effect to speak of.

It would thus appear that both specific binding and network exclusion are contributing to the anti-coagulant effect of hyaluronic acid on thrombin-catalyzed fibrinogen clotting.

Note the quantitative differences between the control experiments of each set; this is due to the nature of the experiment, which is inherently unrepeatable in some aspects. The fibrinogen and thrombin were obtained from an industrial source and complete uniformity of the reagents cannot be assumed. In addition, thrombin settles out of its solution over time resulting in slightly greater or slightly less amounts of thrombin being delivered to different experimental solutions. What is important is that *within each set* the nature of the reaction does not change, and a control performed at the beginning of the session yields similar results to a control performed at the end of the session. This being the case, results from different experimental sessions can be compared on a purely qualitative basis; that is, since the results are normalized by the control, it is each experiment's relation to its control that provides the useful information.

4. GUM SYNERGISM AND SYNTHETIC REPLACEMENTS FOR SYNOVIAL FLUID

4.1 INTRODUCTION

Synovial fluid bathes the large articular joints of the human frame, providing a cushion between joints that acts both as a shock absorber and lubricant. Hyaluronic acid is the polymeric component of synovial fluid most responsible for these unique rheological properties; not surprisingly, when the hyaluronic acid of a joint becomes degraded, the fluid cannot adequately prevent bones from knocking and rubbing together. Indeed, it has been found that the synovial hyaluronic acid in individuals suffering from osteoarthritis is in a degraded state, with a lower average molecular weight than normal. One therapy for osteoarthritis is viscosupplementation: the injection of high-molecular weight hyaluronic acid directly into a joint in order to restore the natural rheology of the synovial fluid.

Viscosupplementation is an effective therapy, providing pain relief and restoration of full motion to partially immobilized joints, but the effects are only temporary. Repeating the procedure on a regular basis would not be more than an inconvenience were it not for the high price of hyaluronan solutions, making this treatment infeasible for the average patient. One possible way to utilize viscosupplementation while circumventing the high cost of hyaluronic acid is to

develop a synthetic fluid that mimics the rheology of a hyaluronic acid solution, but at a fraction of the cost.

The requirements that such a viscosupplement must meet include: affordable cost; longevity in the joint environment; biocompatible with the human body; and able to match performance of hyaluronic acid in both shear flow and elongational flow.

Biopolysaccharides, such as xanthan gum, show some promise in meeting these goals. As a family they are relatively inexpensive, they are stable at the pH found in the joint environment, and they are already cleared for consumption by the FDA. The question remains as to whether a biopolysaccharide solution can meet the demanding rheological requirements. Fortunately, the flow properties of most biopolysaccharide solutions can be fine-tuned to a large degree by utilizing the phenomena of synergism, where a combination of gums exhibits dramatically different flow properties than either gum alone. The final applicable behavior of gum solutions is also strongly affected by the temperature conditions under which the solution was processed. It therefore seems possible that a gum solution can be engineered to meet all of the above-mentioned requirements.

4.2 LITERATURE REVIEW

4.2.1 Viscosupplementation

As noted in Chapter 2, hyaluronan solutions exhibit ideal material properties for a lubricating and shock-absorbing medium within synovial joints. The viscoelastic nature of HA solutions allows for elastic responses (absorbing force during sudden joint compression) as well as viscous responses (providing lubrication for the normal swing of a joint). They are obviously very non-Newtonian in nature, with a high viscosity at low rates of shear and relatively low viscosity at higher rates of shear.

Many researchers believe that HA plays such a critical role in the rheology of synovial fluid that its degradation results in severe consequences for the joint (Ogston & Stanier, 1953; Johnston, 1954; Balazs, 1982). Indeed, it has been found that the HA in osteoarthrotic joints is of lower molecular weight and in lower concentration than the HA in healthy joints, resulting in decreased viscosity and elasticity (Balazs et al. 1967; Balazs 1982). The cushioning and lubricating role of the synovial fluid is compromised, leading to increased bone contact and wear (Murakami et al., 1998).

Rydell and Balazs (1971) proposed that solutions of high molecular weight HA might provide relief when injected directly into joints affected by osteoarthritis; the theory of "viscosupplementation." Their first published study on the effectiveness of viscosupplementation seemed to indicate that this might be a promising approach. Animals suffering from osteoarthritis were treated with solutions of HA (molecular weight ≈ 1 to 2 million Da), with concentrations 3 – 8 mg/ml. Dogs, rabbits and owl monkeys with damaged joints showed a statistically significant increase in their rates of recovery when treated with intra-articular injections, as compared to those who did not receive the treatment. The effect, if any, that solution concentration has upon the healing process was not determined.

Peyron and Balazs (1974) shortly thereafter proceeded with human viscosupplementation studies. Solutions of HA (molecular weight ≈ 1 to 2 million Da) with a concentration of 10 mg/ml were injected directly into the osteoarthritic joints of affected humans. As with the animal studies, a statistically significant percentage of subjects experienced definite improvement when treated with HA, as compared to those who received a placebo. No serious side effects were noted.

This apparent success prompted much subsequent research on viscosupplementation with HA and crosslinked HA derivatives, the general results of which have been summarized by Denlinger (1998) and Adams (1998); the

consensus is that the procedure is a beneficial one, with the following caveats: 1) The relief obtained via viscosupplementation is only temporary, with the painful symptoms of arthritis returning sometimes in a matter of days, sometimes in a matter of months, 2) Crosslinked HA derivatives appear to provide longer lasting relief, on the order of months, perhaps due to their longer residence time within the joint, and 3) Crosslinked products are typically more expensive than "natural" products, adding to the burden of a procedure that is already expensive enough to put it out of the reach of those without a co-operative health plan.

4.2.2 The Active Component of Synovial Fluid

It should be noted at this point that there is some debate as to whether HA is the component of synovial fluid most responsible for its flow properties. Radin and colleagues (1970) separated HA from synovial fluid and reported that solutions of HA are "markedly inferior to synovial fluid as joint lubricants" and "the joint lubricating fraction of bovine synovial fluid is therefore a protein or glycoprotein which is free of hyaluronate." This study is often quoted by those who do not believe that HA plays a significant role in synovial fluid rheology. On the other hand, Balazs and Sundblad (1959) found no significant difference between the viscosities of HA solutions and the viscosities of HA-containing synovial fluid. The difference may lie in how the HA was isolated. Balazs and Sundblad utilized electrodeposition, while Radin et al. (1970) used cesium chloride density gradient

centrifugation, a procedure for HA isolation in wide use at the time (Silpananta et al., 1967; Scher & Hamerman, 1972). Altmann and Zeidler (1982) have subsequently reported, however, that cesium chloride centrifugation appears to irreversibly degrade the HA during the isolation process. The results obtained by Radin must therefore be viewed with a skeptical eye.

4.2.3 Synthetic Products for Viscosupplementation

While viscosupplementation using HA and HA-derivatives has received much attention and research, the notion of a *synthetic* replacement for synovial fluid has largely been ignored. Very little literature exists that addresses this possibility; the most thorough work being that of Helal and Karadia (1968) who used silicone oil in a clinical viscosupplementation trial. The authors reported good results—on a somewhat qualitative basis—when silicone oil was introduced to rheumatic and osteoarthritic joints, inspiring them to perform a large scale clinical trial involving 1 000 arthritic joints (Helal et al., 1970) which eventually provided equally encouraging results. The trials conducted by Helal and Karadia (1968) were uncontrolled and, as mentioned, more qualitative than might be desired. Controlled work subsequently performed by Wright et al. (1971) and Corbett et al. (1970) seemed to indicate that silicone oil had no more than a placebo effect.

Nuki et al. (1969) attempted to duplicate the rheological properties of synovial fluid with solutions of polyvinyl-pyrrolidone (PVP). PVP was chosen because it is water soluble, physiologically compatible with the human body, and because its viscosity is somewhat comparable to that of healthy synovial fluid.

PVP normally displays Newtonian behavior, which is unsatisfactory if one is attempting to duplicate the properties of synovial fluid, which is highly non-Newtonian. Irradiating samples of PVP in a nuclear reactor, however, was found to induce the formation of side chains (Wilson, 1965), resulting in more non-Newtonian flow behaviors. The authors concluded that a solution of irradiated PVP "seems to satisfy the rheological criteria for a synthetic synovial fluid."

The veracity of this statement is debatable; at all shear rates the viscosity of the researcher's PVP solution was considerably higher than the viscosity of synovial fluid. On a plot of apparent viscosity versus shear rate, the curves for PVP and synovial fluid are closest at the lowest shear rate (10^{-2} s^{-1}): approximately 30 poise for synovial fluid and approximately 100 poise for PVP. The greatest deviation occurs at the highest shear rate (10^{2} s^{-1}): approximately 0.2 poise for synovial fluid and approximately 7 poise for PVP. This is a considerable difference. It should also be noted that, in general, solutions of irradiated PVP are not nearly as shear-thinning as synovial fluid. Furthermore, no dynamic experiments were performed

by the research group, precluding the comparison of storage and loss moduli between PVP and synovial fluid.

After the work of Nuki et al. (1969) was published, interest in synthetic replacements seemed to disappear and little more of value can be found in the literature.

4.2.4 Gum Synergism

4.2.4.1 Xanthan Gum

Xanthan gum is an anionic polysaccharide, secreted by the bacterium *Xanthomonas campestris, Xanthomonas phaseoli, and Xanthomonas juglandis* (Harada, 1992; Morris el al., 1977), that has found great utility in the food industry, thanks to its unusual rheological properties.

Being a well-studied polysaccharide, the structure of xanthan gum has received much scrutiny. It is known that the backbone consists of β-(1→4)-D-glucose repeating units, substituted at C-3 on alternating glucose residues with a trisaccharide chain—two mannose units with a glucuronic acid unit between them (Jansson et al., 1975; Melton et al., 1976). The side chain itself may have a pyruvic acid residue on the terminal mannose unit, and it may have an acetyl group at the non-terminal mannose unit; the degree of these substitutions varies with the different substrains of bacterium (Sandford et al., 1977).

Less is known of the secondary structure of xanthan gum in solution, and controversy surrounds the existing theories. Optical rotation studies have shown that xanthan can undergo an "order-disorder" transition under certain conditions, related to the temperature, pH, and ionic strength of the solution (Holzworth, 1976;

Milas & Rinaudo 1979; Norton et al., 1984), where "disorder" here implies a random coil morphology and "order" implies a helix. The question is whether the coil is single- or double-stranded; there is, unfortunately, ample evidence supporting both possibilities. Milas et al. (1988) report that electron microscopy data seems to support a single-stranded helix.

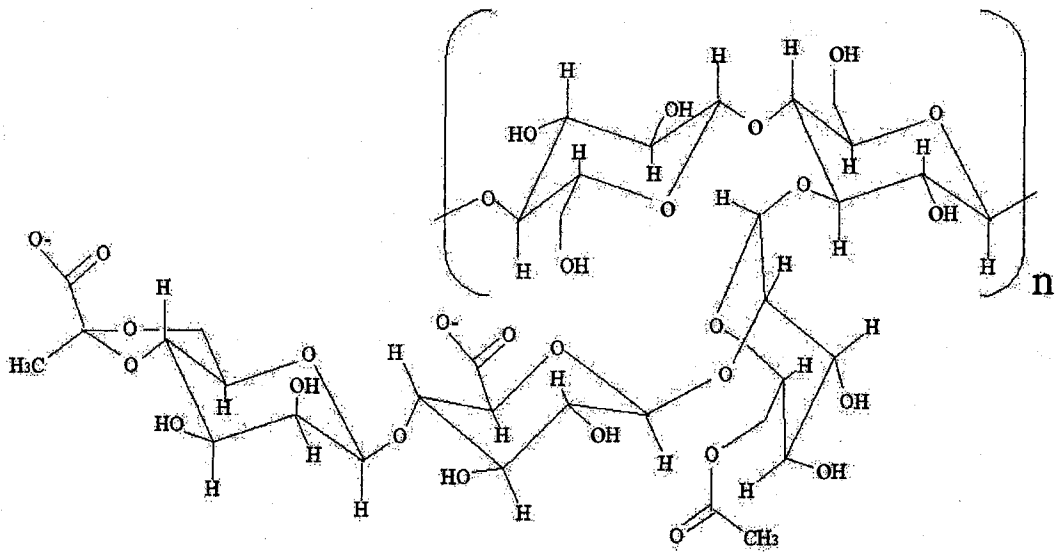

FIGURE 4.1: Structure of the xanthan gum repeat unit

4.2.4.2 Gellan Gum

Gellan gum is an anionic, extracellular polysaccharide secreted by the bacterium *Pseudomonas elodea.* The backbone repeat unit is a tetrasaccharide composed of three D-glucose units followed by an L-rhamose unit, the glucose units being linked β-(1→4) while the rhamose hooks up to the terminal glucose α-(1→4) and to the leading glucose as β-(1→3) (O'Neill et al., 1983; Jansson and Sandford, 1983).The backbone can be substituted at the leading glucose unit; at C-2 with L-glycerate and at C-6 with acetate (Moorhouse et al., 1981). X-ray diffraction studies support the notion of a threefold double-stranded helix conformation for gellan gum in solution (Attwool et al. 1986).

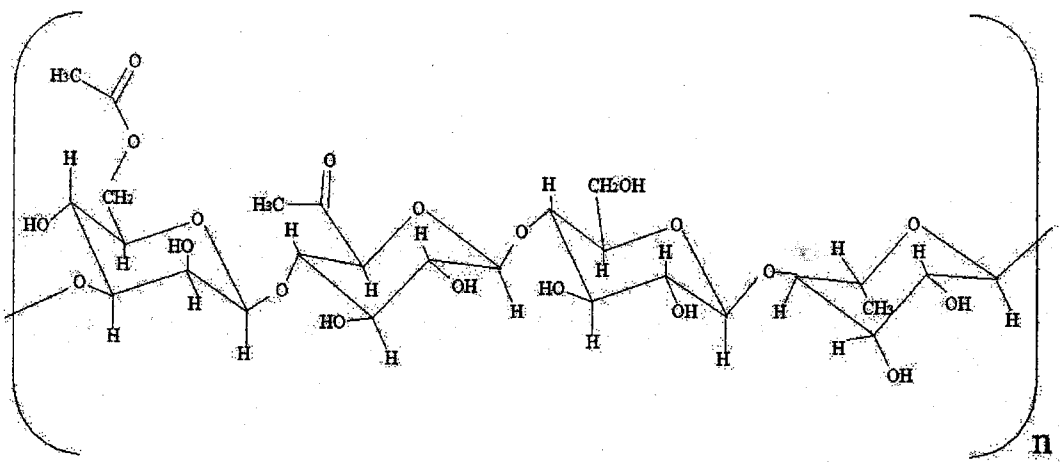

FIGURE 4.2: Structure of the gellan gum repeat unit

4.2.4.3 Locust Bean Gum

Locust bean gum is a member of the galactomannan family, polysaccharides which share a similar backbone of β-(1→4)-D-mannose units, partially substituted at the C-6 position with α-linked D-galactose units. The sole difference between the members of the galactomannan family is the degree of this substitution, reported as a ratio of mannose to galactose (M:G). Dea and Morrison (1975) determined that locust bean gum has a M:G ratio of 3.5:1.

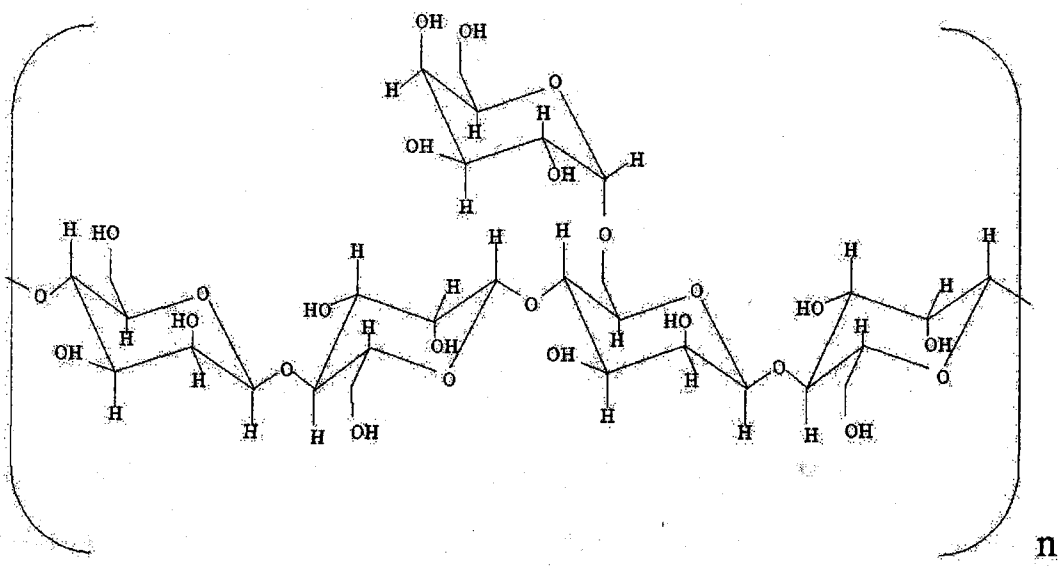

FIGURE 4.3: Structure of the locust bean gum repeat unit

4.2.4.4 Synergism Theories

Certain mixed polymer systems exhibit enhanced properties relative to the individual components of the mixture; for example, while neither xanthan gum nor locust bean gum will gel alone, mixtures of the two polysaccharides can indeed gel. Solutions of mixed, synergistic polymers often are more viscous than either polymer would be alone in solution at the same concentration.

Rocks (1971) was the first researcher to publish evidence of synergism between xanthan gum and galactomannans, reporting that xanthan gum and locust bean gum can form thermoreversible gels while xanthan gum and guar gum cannot. Rocks postulated that locust bean gum, with fewer side chains than guar gum, has a configuration more compatible with the xanthan gum molecule.

Dea et al. (1977) studied optical rotation data from xanthan gum and locust bean gum, alone and when mixed together. Locust bean gum shows an optical rotation independent of temperature, while the optical rotation of xanthan gum undergoes a transition indicating the order-disorder conformation change. A mixed system of xanthan gum and locust bean gum exhibits a very similar change in optical rotation, except that the curve is shifted 10°C higher, suggesting that the xanthan helix is stabilized in some manner by the locust bean gum molecule. The authors suggested that the unsubstituted regions of the galactomannan were binding with

the ordered xanthan helix. Galactomannans with lower galactose content, and therefore more "smooth" regions, should therefore show greater interactions with xanthan gum in solution.

McCleary (1979) noted, however, that a galactomannan from the bacterium *Leucaema leucocephala* showed strong interactions with xanthan despite having a galactose content of 38%, similar to guar gum (which does not show strong interactions with xanthan). McCleary showed that the polysaccharide, while not having significant "smooth" regions, did possess long stretches of backbone that were substituted only on one side of the chain. It appears that having one unsubstituted side is sufficient to provide a binding region for the xanthan helix.

McCleary et al. (1984) showed that progressive enzymic debranching of guar gum resulted in xanthan-guar gels with increased gel strength, melting point, and storage modulus, implying that xanthan-galactomannan interactions increase with increasing M:G ratio (though at M:G ratios greater than ~7, galactomannans become increasingly insoluble in water). Further evidence for this hypothesis was supplied by Dea, Clark and McCleary (1986), who report that carob gum (with M:G ratio of 3.5) and tara gum (with M:G ratio of 2.7 – 3.0) produce gels when mixed with xanthan gum, while native guar gum (with M:G ratio of 1.55), does not.

Along the same lines, Lopes et al. (1992) noted that the intermolecular interactions in a xanthan-guar mixed gum system seem to grow in strength when the acetyl group on the xanthan side chain has been removed, suggesting that the deacetylated xanthan exhibits greater flexibility and thus more potential for junction zone interactions. Tako et al. (1984) and Rees (1972) found similar results for deacetylated xanthan/locust bean gum mixtures.

Tako (1991) repeated the optical rotation studies of Dea et al. (1977) and found that the optical rotation of locust bean gum is independent of temperature down to 25°C, below which the optical rotation increases, possibly due to self-aggregation of the molecules. The optical rotation data reported for deacetylated xanthan/locust bean mixtures were essentially identical to that reported for deacetylated xanthan gum alone, expect for 1) the temperature shift as noted by Dea et al. (1997), and 2) below 25°C the optical rotation is higher in the mixture, even after the temperature shift has been accounted for. Tako suggests self-aggregations are occurring alongside the interspecies interactions. Furthermore, Tako notes that the dynamic modulus of xanthan/locust bean mixtures was reduced when urea was present, suggesting that hydrogen bonding is a key part of the interaction. Tako specifically postulated that the mannose residue of the xanthan chain forms a hydrogen bond with the hydroxyl group on an adjacent mannose residue of the locust bean chain.

Morris (1992) and Brownsey et al. (1988) suggest that the xanthan helix must be denatured in order to provoke specific interactions with the locust bean gum molecule. Based on X-ray diffraction data, they propose a xanthan/locust bean binding scheme which sandwiches a "smooth" region of galactomannan between two xanthan molecules with staggered side chains. (The staggered side chains are required in order to explain the measured interplanar spacing of 0.52 nm. If only one xanthan molecule were implicated in the binding, the repeat distance would be 1.04 nm.)

4.3 EXPERIMENTAL BACKGROUND AND THEORY

The phenomena of gum synergism can be used as a tool in modulating solution properties, but the degree of synergism between gums is heavily dependent upon the solvent used.

Anionic polymers behave differently in a saline solution than they will in pure water. Cationic salts neutralize the centers of negative charge along the polymer chain, thereby allowing it to assume a more compact configuration—this has serious effects on solution viscosity, optical rotation, and the interaction between solution components. The importance of salinity in gum synergism therefore cannot be understated in this research, since the end product (a gum solution that

emulates the rheology of synovial fluid) will find its application in a salty environment, i.e. human joints.

Furthermore, the end product will of course be utilized at body temperature. For these reasons, the experiments described below were conducted in a phosphate buffered saline at 37° C. Increased temperature generally leads to increased molecular mobility and decreased viscosity, though increased temperature may also lead to progressive opening of the xanthan gum coil and stronger interactions between gum molecules.

The techniques used to determine rheological behavior are the same used in Chapter 2 to characterize the rheology of HA solutions (see Chapters 2.3.2.2 and 2.3.2.3): constant rate rotational viscometry and oscillatory dynamic mechanical testing.

4.4 METHODS AND MATERIALS

Xanthan gum (under the tradename Keltrol®) and gellan gum (under the tradename KelcoGEL®) were supplied by Kelco Co., locust bean gum (LBG) by Sigma, guar gum by Aldrich, and hyaluronic acid (HA) by Biozyme Laboratories. All materials were used as provided with no modifications.

The saline solution used was a phosphate buffered saline (PBS) designed to mimic the environment found in human articular joints, with regards to pH and osmolality. Its composition is 7.813 mM sodium phosphate dibasic, 21.875 mM sodium phosphate monobasic, and 150 mM sodium chloride in distilled water.

All measurements were taken with a Bohlin CS 50 Controlled Stress Rheometer. Unless otherwise noted, measurements were taken with a cone-and-plate geometry, using a 4° cone with a 40mm diameter. Dynamic mechanical data was gathered at frequencies from 0.1 Hz to 10 Hz, and at strains of 10% and 25%. Constant rate data was gathered at shear rates from approximately 0.1 to 1000 s^{-1}.

4.5 RESULTS AND DISCUSSION

4.5.1 Gum Synergism in Water

In water, many pairs of polysaccharide gums will exhibit synergism in solution, e.g. xanthan and locust bean, xanthan and gellan, xanthan and guar. An example of such gum synergism is shown in Figure 4.4, which displays the flow curves of xanthan gum solutions, gellan gum solutions, and mixtures of the two. There are two interesting observations to be made regarding this graph: 1) that adding even very small amounts of gellan gum to xanthan gum results in noticeably increased viscosity, and, in fact, that using 0.01wt% gellan gum gives results indistinguishable those obtained when using 0.1wt% gellan gum, and 2) that a xanthan/gellan gum mixture has increased viscosity but exhibits the same shear-thinning behavior as gellan gum. At higher shear rates, this actually results in a viscosity that is less than that of a xanthan gum solution minus the gellan gum. This particular form of synergism, in fact, appears to be an excellent way to get the flow characteristics of a very concentrated gellan gum solution, while using only a nominal quantity of gellan gum.

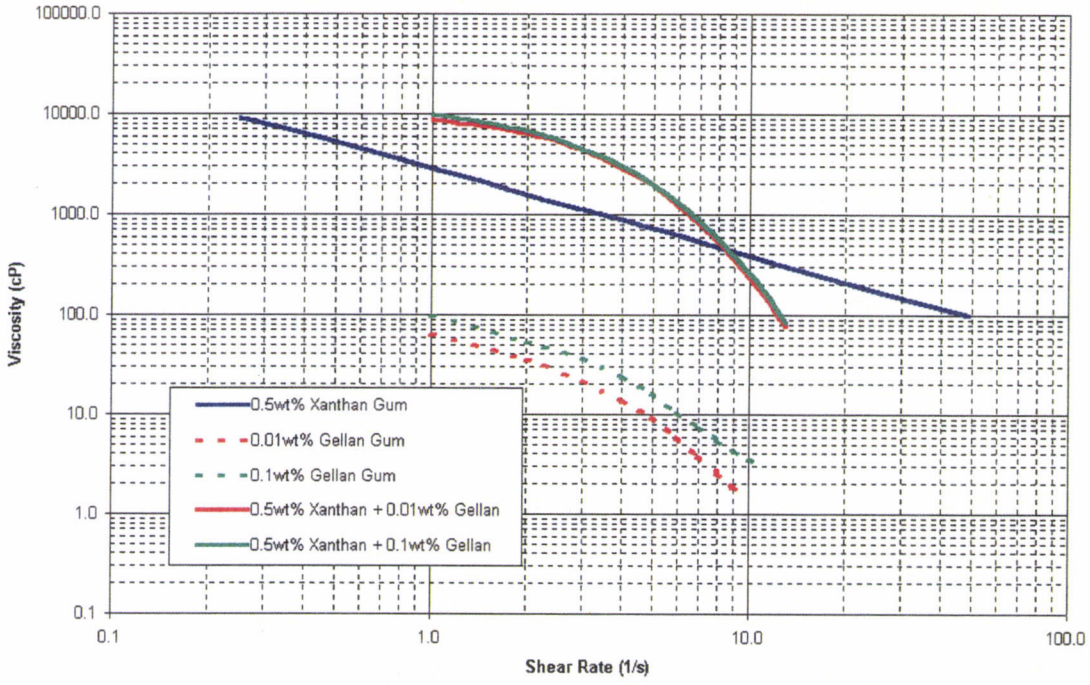

FIGURE 4.4: Demonstration of the synergistic interaction between xanthan gum and gellan gum in aqueous solution at room temperature

4.5.2 Gum Synergism in Saline

Salt-containing solvents tend to disrupt the synergistic interactions between polysaccharides by shielding backbone charges and affecting the polymer morphology in solution. In the case of xanthan gum, it seems that this results in a stabilized helix which is less likely to bind which another polysaccharide molecule. Figures 4.5 and 4.6 are the flow curves for polymer systems (Xanthan/Gellan Gum and Xanthan/Guar Gum) that show synergism in water but fail to exhibit synergism in saline solution.

It appears that at least one mixed system of common gums retains synergistic interactions in saline solution. Figure 4.7 displays the flow curve for a mixture of xanthan gum and locust bean gum in PBS, in comparison with the two gums alone. The result is a solution that behaves as a xanthan gum solution, in terms of the extent of shear-thinning, but at a higher concentration.

The viscoelastic behavior of xanthan/locust bean gum solutions in PBS also indicates the presence of synergistic interactions (Figure 4.8). Both the storage and loss moduli are higher in the case of the mixed gum solutions as compared to the two pure gum solutions. Notice also that the mixed gum solution is clearly gel-like, with G' greater than G" across the whole tested spectrum of frequencies, while the xanthan gum and locust bean gum solutions experience cross-over points.

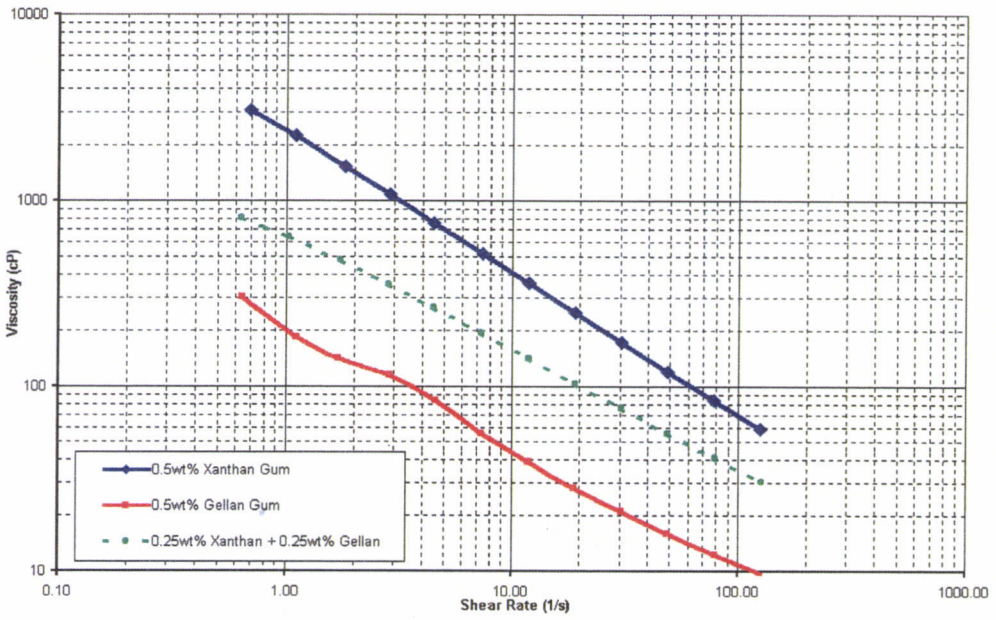

FIGURE 4.5: Demonstration of the absence of synergistic interactions between xanthan gum and gellan gum in PBS at room temperature

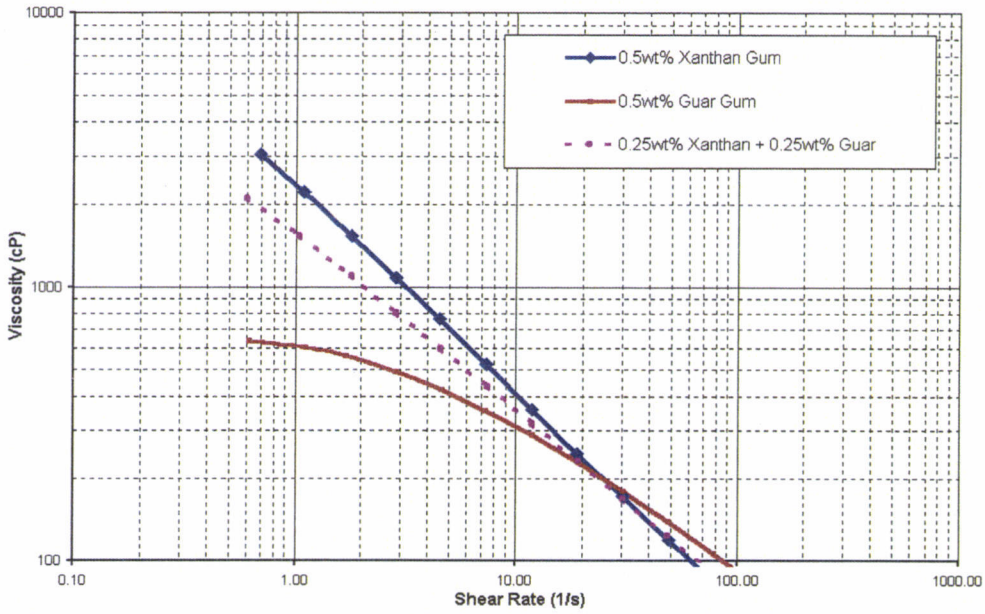

FIGURE 4.6: Demonstration of the absence of synergistic interactions between xanthan gum and guar gum in PBS at room temperature

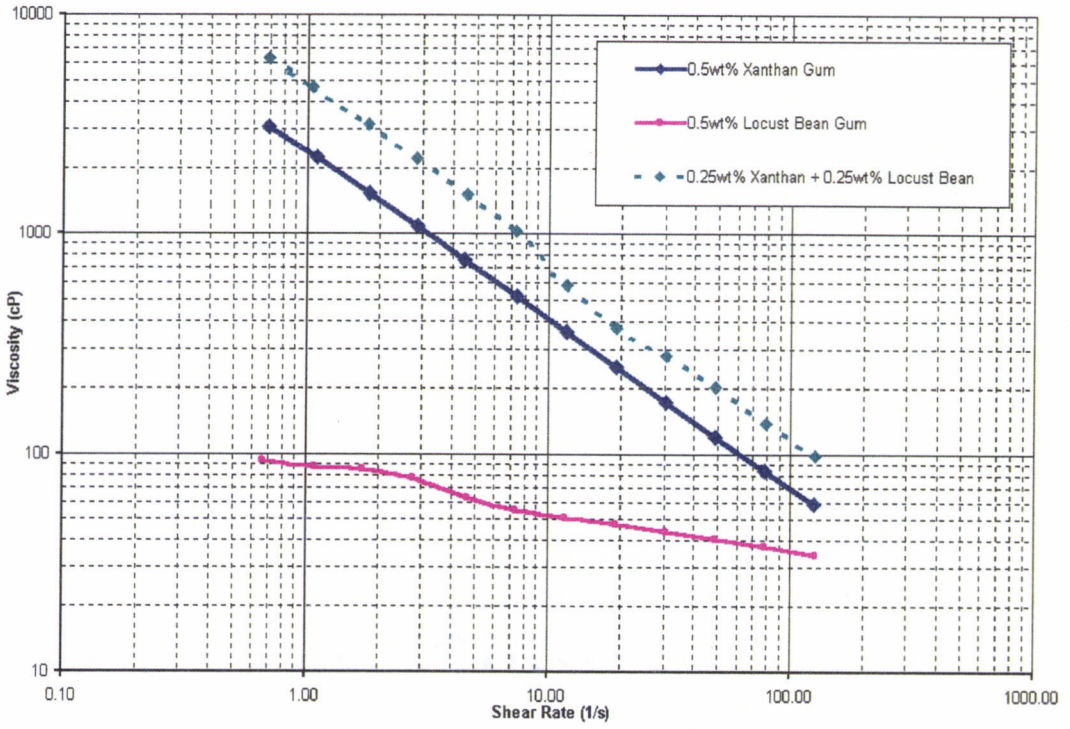

FIGURE 4.7: Demonstration of the synergistic interaction between xanthan gum and locust bean gum in PBS at room temperature

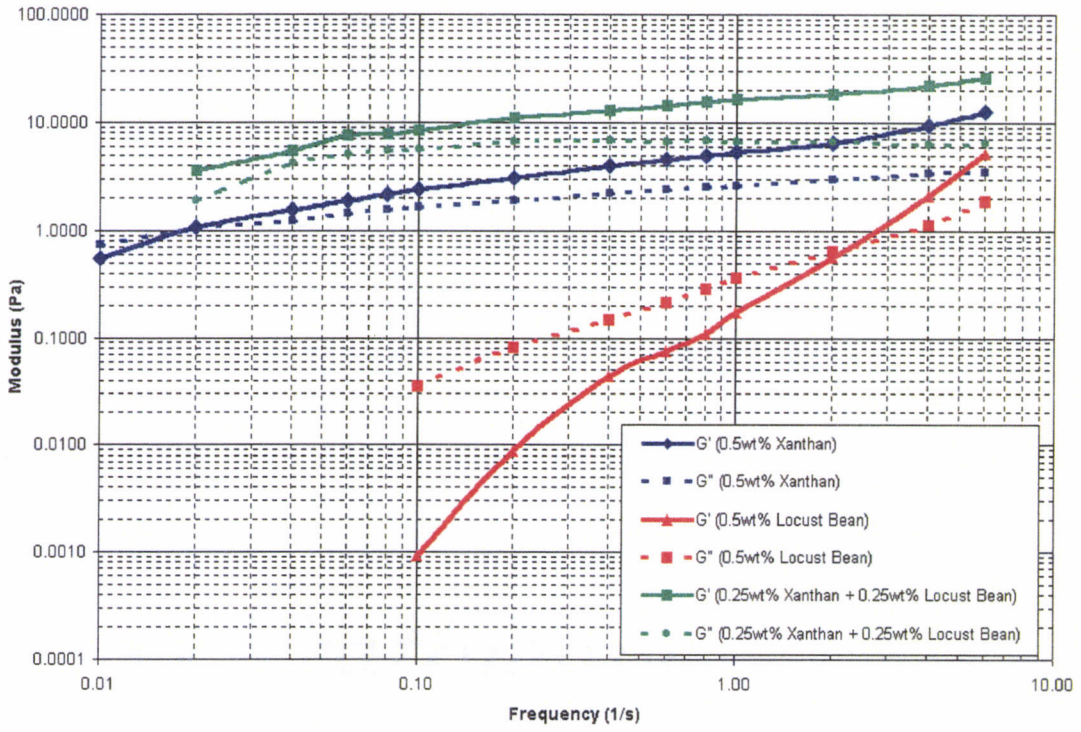

FIGURE 4.8: Dynamic oscillatory shear data from xanthan gum and locust bean gum, alone and mixed, in PBS at room temperature

4.5.3 Mixtures of Xanthan Gum and Locust Bean Gum in PBS

4.5.3.1 Effect of Temperature

It has been shown that xanthan gum and locust bean gum exhibit a synergistic interaction that is not completely disrupted by the presence of salt cations. The aforementioned experiments were performed, however, at room temperature, whereas any therapeutic application of the solution would be utilized at body temperature (37° C). It was important to ascertain what affect the solution temperature has upon the synergistic interaction. As can be seen in Figures 4.9, an increase in temperature of 12° C has a negligible effect on the flow properties of the solution, suggested that the synergistic interaction remains stable.

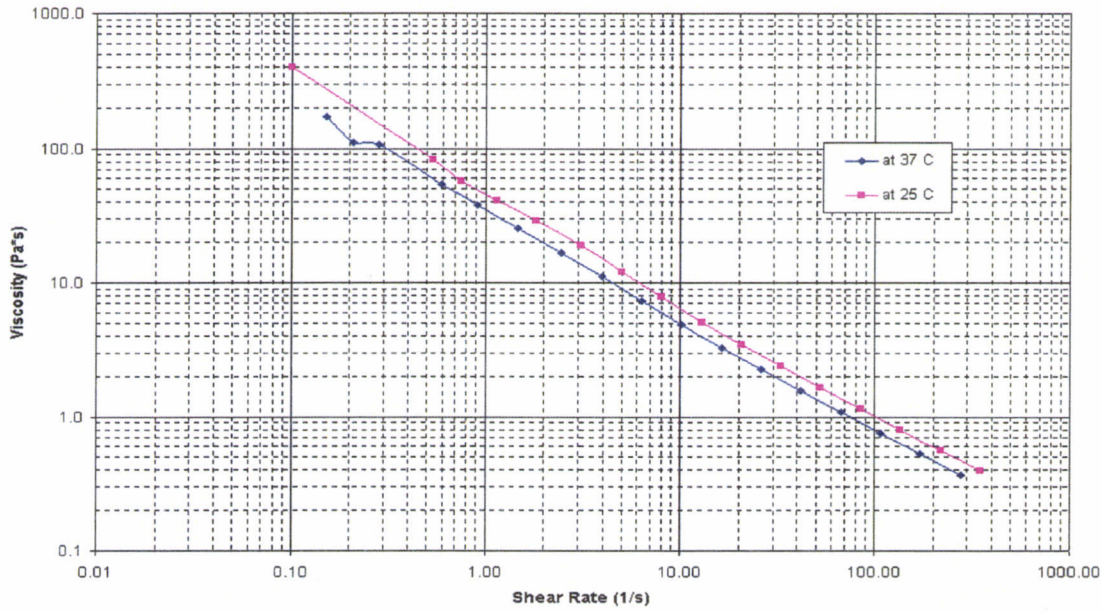

FIGURE 4.9: Effect of solution temperature on flow curve of 0.75wt% xanthan gum, 0.75wt% locust bean gum in PBS

4.5.3.2 Rheology of Mixtures

It has therefore been determined that xanthan and locust bean gums, in a saline solution held at body temperature, continue to show synergistic effects. In Figure 4.10, the flow curves of four 0.75wt% gum solutions are compared. Note that the 0.25wt% XG, 0.5wt% LBG and the 0.5wt% XG, 0.25wt% LBG solutions display similar flow behaviors, though it does appear that the solution with the higher XG concentration is slightly more viscous and shear-thinning, just as the pure XG solution is more viscous and shear-thinning than is the LBG solution. This general behavior of mixed XG/LBG solutions is evident regardless of the concentrations

used. The solution has a greater viscosity than either gum would have alone, and behaves qualitatively like whichever component is present in greater concentration.

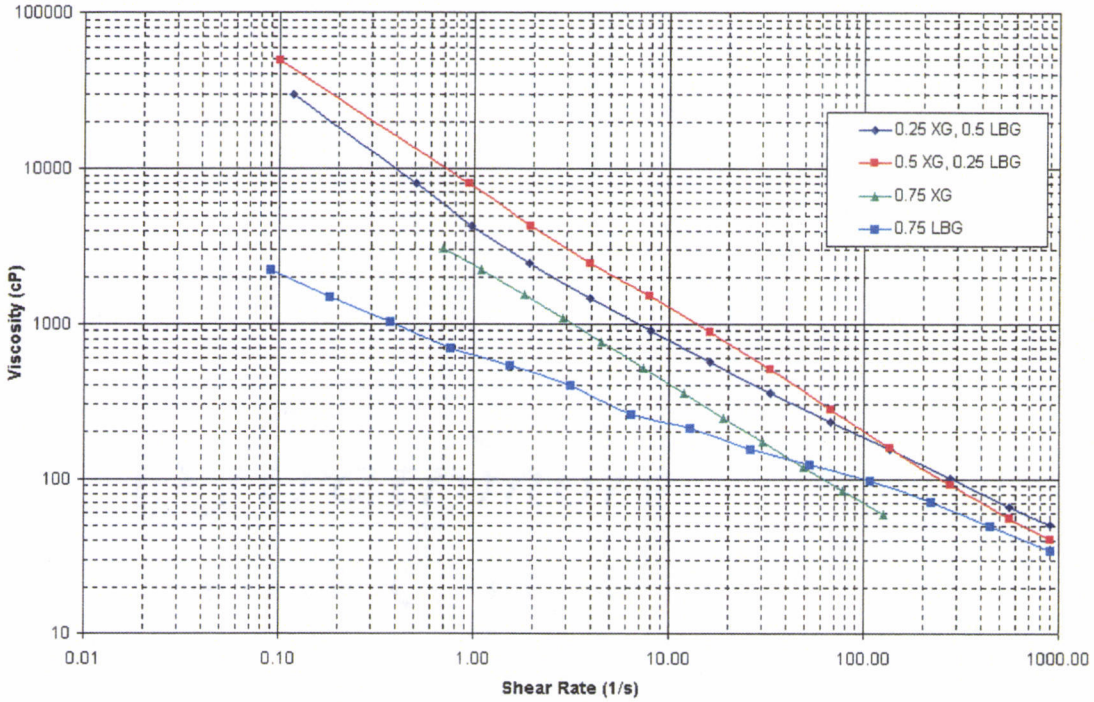

FIGURE 4.10: Flow curve comparison of 0.75wt% gum solutions in PBS at 37° C

4.5.4 Preparing Solutions at Different Temperatures

As can be seen in Figure 4.11, a solution of 0.25wt% XG and 0.25wt% LBG in PBS, prepared at room temperature, does not approximate the viscosity vs. shear rate behavior of a 1wt% HA solution. When the same solution was mixed at higher temperatures (80° and 100° C), allowed to cool and then ran at 37° C, the viscosity increases. In fact, in this manner it is possible to create a 0.25wt% XG, 0.25wt%

LBG solution with a flow curve close to that of 1.0wt% HA. This gives credence to the idea that, at higher temperatures, the xanthan gum helix opens up to some extent, allowing for stronger junction zone interactions with the locust bean gum molecule. It can also be seen that when xanthan gum was heated to 80° or 100° C, cooled to room temperature, and then mixed with locust bean gum in PBS, the solution exhibited increased viscosity. It would seem that xanthan gum which has been sufficiently heated does not return to the original ordered state upon cooling, but rather to an "extended" coil. This is in line with the theory of Milas and Rinaudo (1986), and is supported by the data showing increased synergism under such conditions (as compared to xanthan gum which has not been heated), since an extended coil would be easier for another polysaccharide molecule to bind with than would a condensed coil.

This sort of altered processing also affects the viscoelastic behavior of the solution (Figure 4.12). By mixing the solution at 100° C, it is possible to raise both the G' and the G" of the mixture, brining it closer in line to the magnitude of a HA solution's moduli. Unfortunately, in any case the resulting solution is gel-like in nature and lacking a cross-over point, making it unsuitable for use as a viscosupplement. While HA allows for joint lubrication at lower frequencies and shock absorption at higher frequencies, these mixed gum solutions will behave always as shock absorbers.

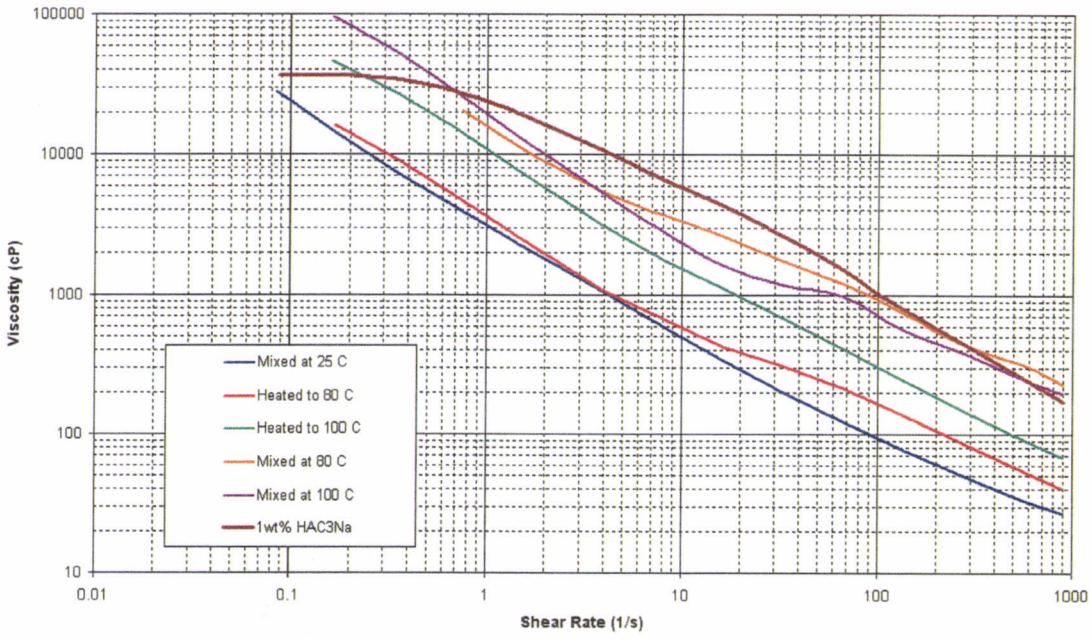

FIGURE 4.11: Flow curves from 0.25wt% xanthan gum, 0.25wt% locust bean gum in PBS at 37° C, prepared at different temperatures, in comparison to a solution of 1wt% HAC3Na in PBS at 37° C

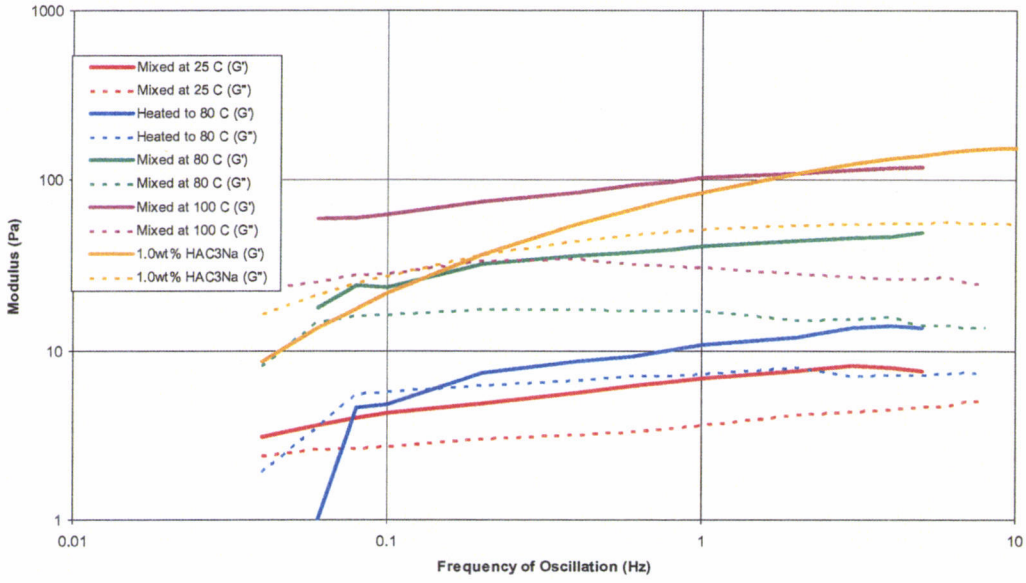

FIGURE 4.12: Dynamic oscillatory shear data, at a strain of 0.25, from 0.25wt% xanthan gum, 0.25wt% locust bean gum in PBS at 37° C, prepared at different temperatures, in comparison to a solution of 1wt% HAC3Na in PBS at 37° C

4.5.5 Replication of the Rheological Properties of Hyaluronic Acid

The experiments detailed above have shown that, by altering the proportions of xanthan gum and locust bean gum in a warm saline solution, the rheological properties of the mixture can be "tuned" over a wide range of behavior, and that polymer usage can be minimized to some degree by taking advantage of the synergistic interaction between the gums. The question remains as to whether enough control can be exerted over the final solution behavior to adequately mimic a clinical-grade preparation of hyaluronic acid. Figures 4.13 and 4.14 present the flow curve and viscoelastic data, respectively, of what the author feels is the XG/LBG system that provided the closest approximation to a 1.0wt% HA solution.

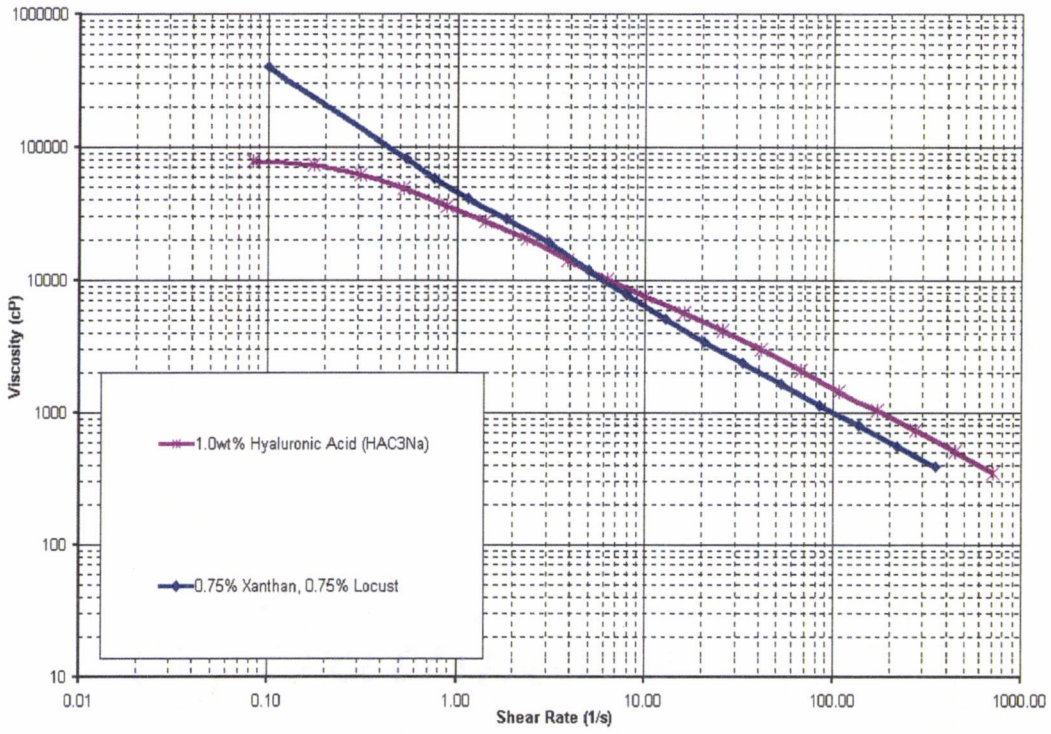

FIGURE 4.13: Flow curve comparison between 1.0wt% HAC3Na in PBS and 0.75wt% xanthan gum, 0.75wt% locust bean gum in PBS

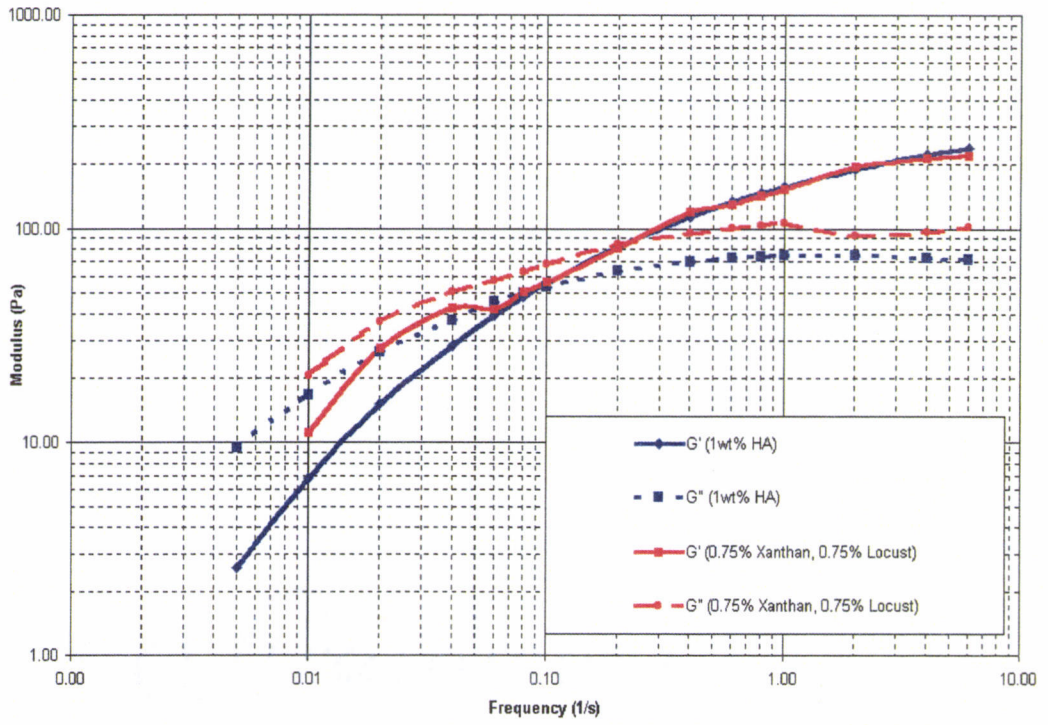

FIGURE 4.14: Dynamic oscillatory shear data comparison between 1.0wt% HAC3Na in PBS and 0.75wt% xanthan gum, 0.75wt% locust bean gum in PBS

While the xanthan/locust bean gum solution does exhibit viscosity of the correct order of magnitude over the range of shear rates studied, note that at low shear rates the curve does not bend over. That is, solutions of hyaluronic acid have a fairly constant viscosity over a range of low shear rates (a "plateau" region) while the viscosity of xanthan/locust bean gum mixtures continues to increases as shear rate is decreased. This would be an unwelcome phenomena were to occur inside a knee joint, where slow bending movements would result in what would likely be perceived as an uncomfortable amount of resistance from within.

Thus, while the viscoelastic properties of an HA solution can be fairly well approximated by a carefully chosen preparation of XG and LBG, the lack of a plateau region in the flow curve renders this concept ultimately inappropriate for the application at hand.

5. SUMMARY OF CONCLUSIONS

Using the technique of multi-angle laser light scattering, the molecular weights of three HA samples were measured. In addition, intrinsic viscosities were measured through dilute solution viscometry, and rheological behavior (flow curves and viscoelastic response) was characterized using constant shear rate and dynamic oscillatory shear rheometry techniques.

Evidence was provided that HA acts to inhibit the formation of thrombin-catalyzed fibrin clot formation, and that it does so through two complimentary mechanisms: an exclusion effect set up by tangled HA networks, and a specific binding between HA and fibrin.

Finally, the author investigated the concept of using synergistic mixtures of polysaccharide gums to mimic the rheological properties of synovial fluid. While many interesting properties of mixed-gum systems were explored, it was eventually determined that the gums used in this study are unsuitable for the purpose at hand.

BIBLIOGRAPHY

Adams, M. (1998) In: Laurent, T.C. (ed) *The Chemistry, Biology and Medical Applications of Hyaluronan and its Derivatives*. Portland Press Ltd., London, U.K.

Altmann, S., Zeidler, H. (1982) Rheologica Acta **21**: 614

Attwool, P., Atkins, E., Upstill, C. (1986) International Journal of Biological Macromolecules **8**: 275

Balazs, E., Sundblad, L. (1959) Acta Soc med Upsaliensis **64**: 137

Balazs, E., Watson, D., Duff, L., Roseman, S. (1967) Arthritis Rheum 10: 357

Balazs, E. (1982) In: Helfet, A. (ed.) *Disorders of the Knee*. J.B. Lippincott Co., Philadelphia

Balazs, E., Leshchiner, A., Leshchiner, A., Band, P. (1987) U.S. Patent No. 4,713,448

Band, P.A. (1998) In: Laurent, T.C. (ed) *The Chemistry, Biology and Medical Applications of Hyaluronan and its Derivatives*. Portland Press Ltd., London, U.K.

Bentley, J.P. (1968) In: Dunphy, J.E., Van Winkle, W. Jr. 0(eds) *Repair and Regeneration.* McGraw-Hill, New York

Bettelheim, F., Bailey, K. (1952) Biochim Biophys Acta **9**: 578

Brownsey, G.J., Cairns, P., Miles, M.J., Morris, V.J. (1988) Carbohydr Res **176**: 329

Campbell, N. (1996) *Biology*. 4th ed. Benjamin/Cummings Publishing Co., Inc., Menlo Park, California, p 834

Carr, M.E. Jr., Shen, L.L., Hermans, J. (1977) Biopolymers **16**: 1

Carr, M.E., Gabriel, D.A. (1980) Macromolecules **13**: 1473

Clark, A.H., Dea, I.C.M., McCleary, B.V. (1986) In: Phillips, G.O., Williams, P.A., Wedlock, D.J. (eds) *Gums and Stabilisers for the Food Industry*, Vol. 3. Elsevier Applied Science Publishers, London, U.K.

Comper, W.D., Laurent, T.C. (1978) Physiological Reviews **58**: 255

Corbett, M., Seifert, M., Hacking, C., Webb, S. (1970) British Medical Journal **1**: 24.

Cowman, M., Liu, J., Li, M., Hittner, D., Kim, J. (1998) Portland Press Ltd., London, U.K., p 17

Dea, I.C.M., Morris, E.R., Rees, D.A., Welsh, E.J., Barnes, H.A., Price, J. (1977) Carbohydr Res **57**: 249

Dea, I.C.M., Morrison, A. (1975) Adv Carbohydr Chem Biochem p. 241

Debye, P. (1944) Appl Phys **15**: 338

Denlinger, J. (1998) In: Laurent, T.C. (ed) *The Chemistry, Biology and Medical Applications of Hyaluronan and its Derivatives*. Portland Press Ltd., London, U.K.

Doolittle, R. (1984) Annu Rev Biochem **53**: 195

Einstein, A. (1910) Ann Phys **33**: 1275

Engstrom-Laurent, A., Laurent, U.B.G., Lilga, K., and Laurent, T.C. (1985) Scand J Clin Lab Invest, **45**: 497

Fouissac, E., Milas, M., Rinaudo, M. (1993) Macromolecules **26**: 6945

Fraser, J.R.E., Laurent, T.C., Engstrom-Laurent, A., Laurent, U.G.B. (1984) Clin Exp Pharm Physiol **11**: 17

Gibbs, D., Merrill, E., Smith, K. (1968) Biopolymers **6**: 777

Harada, T. (1992) Trend Glyco Sci. Glyco Technol. **4**: 309

Hayen, W., Goebeler, M., Kumar, S., Rießen, R., Nehls, V. (1999) Journal of Cell Science **112**: 2241

Helal, B., Karadia, B. (1968) Ann Phys Med **9**: 334

Helal, B., Cozen, L., Kramer, L. (1970) Internat Surg **54**: 317

Holzworth, G. (1976) Biochemistry **15**: 4333

Jansson, P.E., Kenne, L., Lindberg, B. (1975) Carbohydr Res **45**: 275

Jansson, P.E., Lindberg, B., Sandford, P.A. (1983) Carbohydr Res **124**: 135

Johnston, J. (1954) Biochem J **59**: 633

Larsen, N.E. (1998) In: Laurent, T.C. (ed) *The Chemistry, Biology and Medical Applications of Hyaluronan and its Derivatives.* Portland Press Ltd., London, U.K.

LeBoeuf, R.D., Raja, R.H., Fuller, G.M., Weigel, P.H. (1986) Journal of Biological Chemistry **261**: 12586

LeBoeuf, R.D., Gregg, R.R., Weigel, P.H., Fuller, G.M. (1987) Biochemistry **26**: 6052

Lecoutier, J., Chauveteau, G. (1984) Macromolecules **17**: 1340

Lopes, L., Andrade, C., Milas, M., Rinaudo, M. (1992) Carbohydrate Polymers **17**: 121

McCleary, B.V. (1979) Carbohydr Res **71**: 205

McCleary, B. V., Critchley, P., Bulpin, P. V. (1984) European Patent Application No. 0 121 960.

Melton, L.D., Mindt, L., Rees, D.A., Sanderson, G.R. (1976) Carbohydr Res **46**: 245

Milas, M., Rinaudo, M. (1979) Carbohydr Res **76**: 189

Milas, M., Rinaudo, M. (1986) Carbohydr Res **158**: 191

Milas, M., Rinaudo, M., Tinland, B., de Murcia, G. (1988) Polymer Bulletin **19**: 567

Moorhouse, R., Colegrove, G., Sandford, P., Baird, J., Kang, K. (1981) In: Brant, D.A. (ed) *Solution properties of polysaccharides.* ACS Symposium Series, Washington, D.C.

Morris, E.R., Rees, D.A., Young, G., Walkinshaw, M.D., Darke, E. (1977) J Mol Biol **110**: 1

Morris, V.J. (1992) In: Phillips, G.O., Williams, P.A., Wedlock, D.J. (eds) *Gums and Stabilisers for the Food Industry*, Vol. 6. Elsevier Applied Science Publishers, London, U.K.

Mosesson, M.W., Sherry, S. (1966) Biochemistry **5**: 2829

Murakami, T., Higaki, H., Sawae, Y., Ohtsuki, N., Moriyama, S., Nakanishi, Y. (1998) Proc Instn Mech Engrs **212 (H)**: 23

Nemerson, Y., Furie, B. (1980) CRC Critical Reviews in Biochemistry **9**: 45

Norton, I.T., Goodall, D.M., Frangou, S.A., Morris, E.R., Rees, D.A. (1984) J Mol Biol **175**: 371

Nuki, G., Ferguson, J., Boyle, J., Boddy, K. (1969) Nature **224**: 1118

Ogston, A., Stanier, J. (1953) J. Physiol. **119**: 253

O'Neill, M.A., Selvendran, R.R., Morris, V.J. (1983) Carbohydr Res **124**: 123

Peyron, J., Balazs, E. (1974) Path Biol **22**: 731

Radin, E., Swann, D., Weisser, P. (1970) Nature **228**: 377

Raman, C.V. (1927) Indian J Phys **2**: 1

Rees, D. (1972) Biochem J **126**: 257

Rocks, J. (1971) Food Technol. **25**: 22

Rosen, S.L. (1993) *Fundamental Principles of Polymeric Materials*. John Wiley & Sons, Inc., New York, p. 56

Rydell, N., Balazs, E. (1971) Clinical Orthopaedics and Related Research **80**: 25

Sandford, P.A., Pittsley, J.E., Knutson, C.A., Watson, P.R., Cadmus, M.C. (1977) ACS Symp Ser (Amer Chem Soc) p. 192

Scher, J., Hamerman, D. (1972) Biochem J **126**: 1073

Shah, G.A., Ferguson, I.A., Dhall, T.Z., Dhall, D.P. (1982) Biopolymers **21**: 1037

Silpananta, P., Dunstone, J., Ogstone, A. (1967) Biochem J **104**: 404

Tako, M., Asato, A., Nakamura, S. (1984) Agricultural and Biological Chemistry **48**: 2995

Tako, M. (1991) J Carbohydr Chem **10**: 619

Weigel, P.H., Fuller, G.M., LeBoeuf, R.D. (1986) Journal of Theoretical Biology, **119**: 219

Weigel, P.H., Frost, S.J., LeBoeuf, R.D., McGary, C.T. (1989) In: Evered, D., Whelan, J. (eds) *The Biology of Hyaluronan.* John Wiley & Sons, Avon, U.K.

Wik, H., Wik O. (1998) In: Laurent, T.C. (ed) *The Chemistry, Biology and Medical Applications of Hyaluronan and its Derivatives.* Portland Press Ltd., London, U.K.

Wilson, H. (1965) Nature **205**: 10

Wright, V. Haslock, D., Dowson, D., Seller, P., Reeves, B. (1971) British Medical Journal **2**: 370

Wyatt, P.J. (1993) Ana Chim Acta **272**: 1

Zimm, B.H. (1948) J Chem Phys **16**: 1093